University of Nevada, Reno

Molecular Identification of Plant Pathogens Affecting *Cannabis sativa* Crops in Nevada

A thesis submitted in partial fulfillment of the requirements for the degree of Master of Science in Cellular and Molecular Biology

by Jennifer L. Schoener

Dr. Dylan Kosma/ Thesis Advisor

Dr. Shouhua Wang/Thesis Co-Advisor

May 2021

THE GRADUATE SCHOOL

We recommend that the thesis
prepared under our supervision by

JENNIFER SCHOENER

entitled

Molecular Identification of Plant Pathogens Affecting Cannabis sativa Crops in Nevada

be accepted in partial fulfillment of the
requirements for the degree of

MASTER OF SCIENCE

Dylan Kosma, Ph.D
Advisor

Shouhua Wang, Ph.D
Co-advisor

Juan Solomon, Ph.D
Graduate School Representative

David W. Zeh, Ph.D., Dean
Graduate School

May, 2021

ABSTRACT

Cannabis sativa L. is an herbaceous flowering plant in the family *Cannabaceae*. *C. sativa* has emerged to be an important economic crop in the United States and is now widely cultivated as hemp for fiber, oil, and seed, and as marijuana (referred to henceforth as cannabis) for medicinal or recreational psychotropic purposes. In Nevada, hemp varieties are generally grown commercially in fields, while cannabis varieties are generally grown indoors. Both types of plants are susceptible to certain diseases, resulting in significant loss of crop yield. To understand hemp pathology and the major pathogens associated with diseases, we investigated the major diseases encountered by farmers and cultivators in Nevada in recent years. Each disease was systemically evaluated to determine the nature of its problem. In order to elucidate the etiology and accurately identify the pathogens that caused the observed diseases, morphological, pathological, and molecular approaches were used. This thesis emphasizes molecular approaches, i.e., DNA barcoding, to identify species based on rDNA sequences and analyzing viral capsid protein gene sequences, which enabled the successful identification of every encountered organism to a species level. The pathogens identified in this study include five *Fusarium* species: *F. oxysporum*, *F. solani*, *F. equiseti*, *F. redolens*, and *F. tricinctum*, two *Alternaria* species: *A. infectoria* and *A. tennuisima*, a powdery mildew fungus*: Golovinomyces ambrosiae*, a virus: *Beet curly top virus,* and a fastidious bacterium; '*Ca*. Phyoplasma trifolii'. These organisms were found to be devastating pathogens of *C. sativa* crops, and they

all were first detected from *C. sativa* crops in Nevada. Correctly identifying pathogens affecting *C. sativa* crops provides a foundation for the management of hemp and cannabis diseases and fills the gap of current information on *C. sativa* pathology.

Acknowledgments

I would like to acknowledge and express gratitude to Dr. Shouhua Wang who has been my mentor in the study of plant pathology and who made this project possible. I would like to express my gratitude to my advisors and committee members: Dr. Dylan Kosma, Dr. Juan Solomon, and Dr. Patricia Santos.

I would also like to thank the Nevada Department of Agriculture plant pathology team: To our lab director Dr. Wang who has guided us in this work, to Russell Wilhelm for performing and assisting in hemp field surveys, to Jenna Gortari for her help in the lab and for the occasional sympathy coffee, and to Patrick Schmitz and Rylee Rawson for their assistance during the early stage of the project. This study was conducted at the Nevada Department of Agriculture Plant Pathology lab.

Finally, but certainly no less important, I express my gratitude to my family, loved ones, and Finn for their love and support.

Table of Contents

List of Tables

List of Figures

BACKGROUND

Cannabis sativa L. is an herbaceous flowering plant in the family *Cannabaceae*. *C. sativa* is cultivated as hemp for fiber, oil, seed, and as marijuana (referred to henceforth as cannabis) for medicinal or recreational psychotropic purposes. Hemp and cannabis are both classified as *Cannabis sativa*, a species containing many different varieties. In Nevada, hemp varieties, which are bred for fiber, seed, and/or oil, are generally grown commercially in fields while cannabis varieties, which have high tetrahydrocannabinol (THC) content, are generally grown indoors. Both types of plants can be affected by diseases, resulting in significant losses of crop production.

Cultivation of industrial hemp was first approved in 2014 for the purpose of research and development. The Federal Farm Bill Section 7606 authorizes state agencies to conduct pilot trials to assess crop viability for the creation of an industry in prospective states. In Nevada, the Department of Agriculture administrates and regulates the production of hemp crops. The approval of the 2018 Farm Bill allowed hemp to be cultivated more broadly as a crop. Under section 10113 of the Farm Bill, a hemp plant with a THC content greater than 0.3 percent is not considered as hemp, but as cannabis (marijuana) and subject to federal law. The changes in federal regulations on *C. sativa* crops have enabled more opportunities for researchers to gain a better understanding of this crop and its pathology as the diseases associated with *C. sativa* crops are emerging.

Some earlier literature suggested a number of diseases that affect the production of hemp, including gray mold, stem canker, damping off, assorted leaf spots, root rots, blights, and nematodes (McPartland, 1996), but significant research on hemp pathology has not been done until recently. Since 2018, researchers in Canada have begun to investigate diseases impacting *C. sativa* in British Columbia (Punja, 2021). Plant pathology laboratories across the United States have begun to study hemp pathology with the expansion of the 2018 Farm Bill as described by the disease report progression outlined in the paragraphs below. With hemp and cannabis gaining popularity, more researchers need to study the pathology of *C. sativa*. Additionally, the diseases observed from *C. sativa* may vary by region, as diseases are affected by the local climate and soil conditions. In Nevada, hemp crops face adverse environmental conditions such as persistent drought and alkaline soil (Dollarhide, 1975). Crops under such growth conditions are more prone to infection by pathogens (Argios, 1997; Garrett *et al.,* 2011).

Since 2016, the number of diseases reported on *C. sativa* crops is increasing rapidly as interest in hemp production grows. Many diseases are first reported on *C. sativa* as it is a newly re-emerged crop. The majority of reported pathogens are fungi and oomycetes, with few reports on viruses, viroids, and phytoplasmas (Punja, 2021).

In 2000, hemp canker caused by *Sclerotinia sclerotiorum* was first reported in Alberta, Canada (Bains *et al.*, 2000).

In 2007, several hemp diseases were reported, including witches'-broom disease caused by elm yellows group 16SrV phytoplasma in China (Zhao *et al.*, 2007) and southern blight caused by *Sclerotium rolfsii* in Sicily and southern Italy (Pane *et al.*, 2007).

In 2017, *Pythium aphanidermatum* crown and root rot of hemp was reported in the United States (Beckerman *et al.,* 2017), and the nematode *Meloidogyne javanica* was reported from hemp in China (Song *et al*., 2017).

In 2018, the following diseases were reported: *Pythium ultimum* crown and root rot of hemp in the United States (Beckerman *et al.*, 2018), charcoal rot caused by *Macrophomina phaseolina* on hemp in Southern Spain (Casano *et al.*, 2018), and powdery mildew caused by *Golovinomyces cichoracearum sensu lato* on cannabis in Canada (Pépin *et al.*, 2018).

In 2019, more diseases were reported: root rot and wilt caused by *Pythium myriotylum* on hemp in the United States (McGehee *et al.*, 2019), crown rot caused by *Sclerotinia minor* on hemp (Koike *et al.*, 2019), foliar blight of hemp caused by *Exserohilum rostratum* (Thiessen and Schappe, 2019), leaf spot caused by *Cercospora cf. flagellaris* in Kentucky (Doyle *et al.*, 2019), and cannabis stunting disease caused by hop latent viroid in California (Bektaş *et al.*, 2019). Pathogens and molds affecting marijuana in Canada were also reported (Punja *et al.,* 2019).

In 2020, additional diseases were reported: *Meloidogyne enterolobii* nematode on hemp in China (Ren *et al.*, 2020), beet curly top virus infecting *C. sativa* in Colorado (Giladi *et al.*, 2020) *Chaetomium globosum* causing leaf spot

on hemp in Tennessee (Chaffin *et al.*, 2020), *Serratia marcescens* causing a leaf spot disease on hemp (Schappe *et al.*, 2020), *Curvularia pseudobrachyspora* and *Cercospora cf. flagellaris* causing leaf spot on hemp in Florida (Marin *et al.*, 2020), *Colletotrichum fioriniae* causing anthracnose leaf spot on hemp (Szarka *et al.*, 2020), *Sclerotium rolfsii* causing southern blight on hemp in Southern Virginia (Amaradasa *et al.*, 2020; Mersha *et al.*, 2020), and *Neofusicoccum parvum* causing dieback and canker on hemp in the United States (Feng *et al.*, 2020).

This study contributes to hemp disease diagnostic research, which leads to a greater understanding of the pathogens affecting *C. sativa* crops. The objective of this study was to gain knowledge of the diseases encountered in *C. sativa* crops in Nevada by accurately identifying associated pathogens through molecular approaches, and thus help to develop better strategies for mitigating diseases.

LITERATURE CITED

Amaradasa, B. S., Turner, A., Lowman, S., & Mei, C. (2020). First report of southern blight caused by *Sclerotium rolfsii* in industrial hemp in southern Virginia. *Plant Disease*. *104* (5), 1563-1563.

Argios, G. N. 1997: *Plant Pathology*, 4th Edition. Academic Press, San Diego.

Bains, P. S., Bennypaul, H. S., Blade, S. F., & Weeks, C. (2000). First report of hemp canker caused by *Sclerotinia sclerotiorum* in Alberta, Canada. *Plant Disease. 84* (3), 372.

Beckerman, J., Stone, J., Ruhl, G., & Creswell, T. (2018). First report of *Pythium ultimum* crown and root rot of industrial hemp in the United States. *Plant Disease. 102* (10), 2045.

Beckerman, J., Nisonson, H., Albright, N. & Creswell, T. (2017). First report of *Pythium aphanidermatum* crown and root rot of industrial hemp in the United States. *Plant Disease. 101* (6), 1038.

Bektaş, A., Hardwick, K. M., Waterman, K., & Kristof, J. (2019). Occurrence of hop latent viroid in *Cannabis sativa* with symptoms of cannabis stunting disease in California. *Plant Disease. 103* (10), 2699.

Casano, S., Hernández Cotan, A., Marín Delgado, M., García-Tejero, I. F. Gómez Saavedra, O., Aguado Puig, A., & de los Santos, B. (2018). First report of charcoal rot caused by *Macrophomina phaseolina* on hemp (*Cannabis sativa*) varieties cultivated in southern Spain. *Plant Disease. 102* (8), 1665.

Casano, A. G., Dee, M. E., Boggess, S. L., Trigiano, R. N., Bernard, E. C., & Gwinn, K. D. (2020). First report of *Chaetomium globosum* causing a leaf spot of hemp (*Cannabis sativa*) in Tennessee. *Plant Disease. 104* (5), 1540.

Dollarhide, W.E., 1975, Soil survey, Fallon-Fernley area, parts of Churchill, Lyon, Storey, and Washoe Counties: Washington D.C., U.S. Department of Agriculture.

Doyle, V. P., Tonry, H. T., Amsden, B., Beale, J., Dixon, E., Li, H., Szarka, D., & Gauthier, N. (2019). First report of *Cercospora* cf. *flagellaris* on industrial hemp (*Cannabis sativa*) in Kentucky. *Plant Disease. 103* (7), 1784.

Feng, C., Villarroel-Zeballos, M. I., Ficheux, P. F., Zima, H., Dhillon, B. D. S. & Correll, J. C. (2020). First report of *Neofusicoccum parvum* causing dieback

and canker disease on hemp in the United States. *Plant Disease. 104* (11), 3075.

Garrett, K.A., Forbes, G.A., Savary, S., Skelsey, P., Sparks, A.H., Valdivia, C., van Bruggen, A.H.C., Willocquet, L., Djurle, A., Duveiller, E., Eckersten, H., Pande, S., Vera Cruz, C. & Yuen, J. (2011), Complexity in climate-change impacts: an analytical framework for effects mediated by plant disease. *Plant Pathology, 60*: 15-30.

Giladi, Y., Hadad, L., Luria, N., Cranshaw, W., Lachman, O., & Dombrovsky, A. (2020). First report of beet curly top virus infecting *Cannabis sativa* in western Colorado. *Plant Disease. 104* (3), 999.

Koike, S. T., Stanghellini, H., Mauzey, S. J., & Burkhardt, A. (2019). First report of sclerotinia crown rot caused by *Sclerotinia minor* on hemp. *Plant Disease. 103* (7), 1771.

Marin, M. V., Coburn, J., Desaeger, J., & Peres, N. A. (2020). First report of cercospora leaf spot caused by *Cercospora* cf. *flagellaris* on industrial hemp in Florida. *Plant Disease. 103* (7), 1784.

Marin, M. V., Wang, N.-Y., Coburn, J., Desaeger, J. & Peres, N. A. (2020). First report of *Curvularia pseudobrachyspora* causing leaf spot on hemp (*Cannabis sativa*) in Florida. *Plant Disease. 104* (12), 3262.

McGehee, C. S., Apicella, P., Raudales, R., Berkowitz, G., Ma, Y., Durocher, S., & Lubell, J. (2019). First report of root rot and wilt caused by *Pythium myriotylum* on hemp (*Cannabis sativa*) in the United States. *Plant Disease. 103* (12), 288.

McPartland, J. M., (1996). A review of Cannabis diseases. *Journal of the International Hemp Association 3* (1), 19-23.

Mersha, Z., Kering, M., & Ren, S. (2020). Southern blight of hemp caused by *Athelia rolfsii* detected in Virginia. *Plant Disease. 104* (5), 1562.

Pane, A., Cosentino, S. L., Copani, V., & Cacciola, S. O. (2007). First report of southern blight caused by *Sclerotium rolfsii* on hemp (*Cannabis sativa*) in Sicily and southern Italy. *Plant Disease. 91*(5), 636.

Pépin, N., Punja, Z. K., & Joly, D. L. (2018). Occurrence of powdery mildew caused by *Golovinomyces cichoracearum* sensu lato on *Cannabis sativa* in Canada. *Plant Disease. 102* (12), 2644.

Punja Z. K. (2021). Emerging diseases of Cannabis sativa and sustainable management. *Pest Management Science*, 10.1002/ps.6307. Advance online publication. https://doi.org/10.1002/ps.6307

Punja, Z. K., Collyer, D., Scott, C., Lung, S., Holmes, J., & Sutton, D. (2019). Pathogens and molds affecting production and quality of *Cannabis sativa L. Frontiers in Plant Science*, 10: 1120.

Ren, Z., Chen, X., Luan, M., Guo, B., & Song, Z. (2020). First Report of *Meloidogyne enterolobii* on industrial hemp (*Cannabis sativa*) in China. *Plant Disease. 105* (1), 230.

Schappe, T., Ritchie, D. F., & Thiessen, L. D. (2020). First report of *Serratia marcescens* causing a leaf spot disease on industrial hemp (*Cannabis sativa*). *Plant Disease. 104* (4),1248.

Song, Z. Q., Cheng, F. X., Zhang, D. Y., Liu, Y., & Chen, X. W. (2017). First report of *Meloidogyne javanica* infecting hemp (*Cannabis sativa*) in China. *Plant Disease. 101* (5), 842.

Szarka, D., McCulloch, M., Beale, J., Long, S., Dixon, E., & Gauthier, N. (2020). First report of anthracnose leaf spot caused by *Colletotrichum fioriniae* on hemp (*Cannabis sativa*). *Plant Disease. 104* (5), 1560.

Thiessen, L. D. & Schappe, T. (2019). First report of *Exserohilum rostratum* causing foliar blight of industrial hemp (*Cannabis sativa*). *Plant Disease. 103* (6), 1414.

Zhao, Y., Sun, Q., Davis, R. E., Lee, I.-M. & Liu, Q. (2007). First report of witches'-broom disease in a *Cannabis* spp. in China and its association with a phytoplasma of elm yellows group (16SrV). *Plant Disease. 91* (2), 227.

Chapter One:

The molecular identification of *Fusarium* species associated with hemp root rot based on the ITS region of rDNA.

ABSTRACT

Industrial hemp (*Cannabis sativa* L.) is an emerging crop in Nevada. In the late summer of 2016, high mortality of up to 70% of plants was observed in a hemp field in Nevada. In three hemp varieties planted, the “Canda” variety was most affected followed by the “Futura-75” and “Joey”. Symptomatic plants exhibited wilt, yellowing, rapid death, and extensive root rot with little lateral root growth. Selected root tissue from 17 symptomatic hemp plants was surface sterilized, placed onto potato dextrose agar amended with streptomycin sulfate, and incubated at 22°C in the dark. DNA was extracted from each of the 34 root fungal isolates followed by PCR amplification of the ITS region of fungal rDNA. Twenty-eight representative *Fusarium* isolates were obtained and sequence analysis of the ITS region of fungal rDNA classified these 28 isolates into five species, namely, *F. oxysporum*, *F. solani*, *F. redolens*, *F. tricinctum*, and *F. equiseti*.

INTRODUCTION

The genus *Fusarium* contains important plant pathogenic fungi with a broad range of hosts and infection strategies (Di Pietro *et al*., 2003; Goswami & Kistler, 2004). Species in this genus can cause significant damage to numerous plant species by infecting seedlings, roots, and crowns (Coleman, 2016).

During the summer of 2016, an industrial hemp crop in Humboldt County exhibited large patches of plant death, affecting up to 70% of the hemp plants in the field (Fig.1-1). Affected plants ceased growth and died rapidly. Surviving plants exhibited yellowing foliage and loss of growth vigor. Infected plants were easily pulled out from the ground, with little to no lateral root growth. Some affected plants had small patches of magenta discoloration on tap roots. Of three hemp varieties planted, the “Canda” variety was mostly affected followed by the “Futura-75” and “Joey”. Seventeen symptomatic plants were collected from the field and examined further in the lab where pathogen identification was then performed.

To identify pathogens isolated from plant tissue, molecular methods were employed. The most common DNA barcode region used for fungal identification is the rDNA Internal transcribed spacer (ITS) region. (Schoch *et al*., 2012; Bellemain *et al*., 2010; Badotti *et al*., 2017). The ITS1 region is located between the 18S and 5.8S rRNA genes, while ITS2 is between 5.8S and 28S rRNA genes. The ITS1 primer (5’-TCCGTAGGTGAACCTGCGG-3’), and ITS4

primer (5’-TCCTCCGCTTATTGATATGC-3’) were used to amplify the specific region (White *et al.*, 1990).

Here, we report our findings that five *Fusarium* species were associated with the root rot and sudden death of an industrial hemp crop, and that *Fusarium oxysporum* was the most prevalent species recovered from infected root tissue. Identification of all associated pathogens helps to better understand this disease and provide valuable information to be used for the effective treatment of the disease.

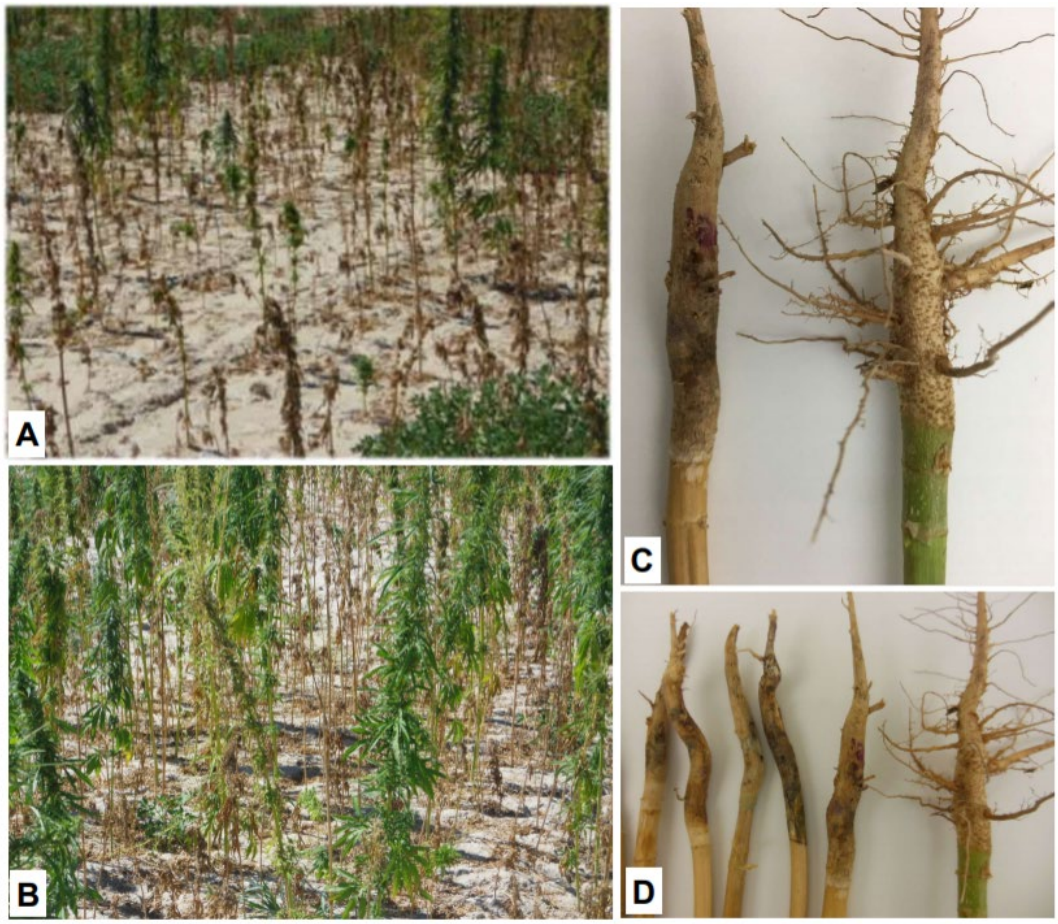

Figure 1-1. High mortality of hemp plants observed in a hemp field found to be caused by an extensive root rot. A. Disease patch observed in an affected field showing rapid death of the majority of hemp plants. **B.** A low percentage of surviving plants in the field appeared healthy but exhibited reduced size and decreased growth vigor. **C.** Symptomatic root showing the observed magenta spots (left) compared to a healthy root (right). **D.** Almost all symptomatic plants pulled from the affected field showed extensive root rot and limited lateral root growth. (Photo by Shouhua Wang)

MATERIALS AND METHODS

Collection of symptomatic plants and preparation of sub-samples. Seventeen hemp plants that represented a variety of symptoms were collected randomly from diseased patches in field by inspectors and examined in lab for etiological evaluation. The symptoms of the collected plants ranged from leaf yellowing, dieback, wilting, to root rot. Symptomatic plants were stored at 5°C temporarily until processing. The root system was cut off from the plant, washed under running tap water, and blotted dry on a layer of clean paper towels. The cleaned roots were then proceeded to tissue cutting for fungal isolation.

Fungal isolation from root tissue. Five small (approx. 3 mm^2) tissue pieces were cut from the affected root tissue of each symptomatic plant by using sterile razors to cut sections from the juncture of visually healthy and diseased root tissue. The excised root tissue pieces were surface disinfected (inside a biosafety cabinet) by soaking them in a 1% sodium hypochlorite (NaOCl) solution for one minute in one quadrant of a quad petri dish followed by rinsing in sterile water for 45 seconds in each of the remaining three quadrants before being blotted on heat-sterilized filter paper to dry. The tissue pieces were then plated on a potato dextrose agar (PDA) media amended with 100 µg/ml of streptomycin sulfate (PDA+Streptomycin). Plates were sealed with parafilm and incubated upside down in the dark at 22°C. Once fungal colonies began to grow on plates, they were further transferred to new PDA media plates to obtain a pure culture.

After purifying each fungal colony through a series of transferring hyphae tips, isolates with distinct morphology were maintained on PDA slants.

DNA extraction from fungal mycelium. Mycelia were excised from the fungal colonies with a sterilized scalpel. Approximately 200 mg of fungal mycelia were collected into a sterile 1.5 ml Lysing Matrix A tube and stored at -20°C for later DNA extraction.

Fungal DNA extraction was performed using Plant DNeasy kits (Qiagen, Germantown, MD) as follows: Four hundred microliters of buffer AP1 and 4 µl RNase A were added to the Lysing Matrix A tubes containing fungal mycelia. Sample tubes were then mechanically homogenized using a Qbiogene FastPrep-24 at speed 6 for 40 seconds. Tubes were incubated in a Thermomixer at 65°C and 300 rpm for 10 minutes. After incubation 130 µl buffer P3 was added to each tube, vortexed to mix, and incubated in ice for 5 minutes. Tubes were centrifuged at 14,000 rpm for 5 minutes to collect tissue sediment at the base of the tube. The resulting lysate was pipetted into a QIAshredder spin column placed in a 2 ml collection tube and centrifuged at 14,000 rpm for 2 minutes. The lysate of each sample was pipetted into a new sterile 1.5 ml microcentrifuge tube. One-and-a-half volume of the lysate recovered from the previous step of buffer AW1 were added and mixed by pipetting. Six hundred fifty microliters of the mixture were added to a DNeasy mini spin column placed in a 2 ml collection tube and centrifuged for 1 minute at 8,000 rpm. The resulting flow-through was discarded, and the remaining liquid was added to the column for a second round of centrifuging at 8,000 rpm for 1 minute. The column of each sample was then

transferred to a new 2 ml collection tube and 500 µl of buffer AW2 was added and tubes were centrifuged for 1 minute at 8, 000 rpm. The flow-through was discarded and another 500 µl of buffer AW2 was added and tubes were centrifuged for 2 minutes at 14,000. Spin columns were placed into new sterile 1.5 ml microcentrifuge tubes and 100 µl of buffer AE was pipetted to the center of each column membrane to incubate for 5 minutes at ambient laboratory temperature, approximately 20-21°C. Columns and tubes were centrifuged for 1 minute at 8,000 rpm to elute DNA in the provided buffer.

PCR amplification of the ITS region of rDNA and electrophoresis. The purified genomic DNA from 34 fungal samples was used to amplify the ITS region of fungal rDNA using primer pair ITS1 (5'-TCCGTAGGTGAACCTGCGG-3') and ITS4 (5'-TCCTCCGCTTATTGATATGC-3') developed by White *et al.*, 1990.

The PCR was performed by assembling the reagents as follows per sample: 5 µl of 10X PCR buffer, 1.5 µl of $MgCl_2$ (50 mM), 1 µl of dNTP mixture (10 mM), 2.5 µl ITS1 primer (10 µM), 2.5 µl ITS4 primer (10 µM), 0.2 µl Platinum *Taq* polymerase, 36.3 µl molecular biology grade sterile water, and 1 µl of template DNA. The PCR reaction master mix was prepared and 49 µl of it was pipetted into each 0.2 ml sterile PCR tube. The DNA template (1 µl) for each sample was added into the PCR tubes, and one microliter of sterile water was added to one PCR tube as a negative control. PCR amplification was performed in a thermocycler with an initial denaturation at 94°C for 2 minutes to completely denature the template DNA and activate the polymerase, followed by 35 cycles

of PCR amplification with the following parameters: 94°C for 1 min denaturation, 58°C strand annealing for 1 minute, strand extension at 72°C for 1 minute. A final extension was performed at 72°C for 10 minutes.

To verify amplification, the PCR products (mixed with loading dye) were loaded into a 1% agarose gel made by adding 1g UltraPure Agarose to 100 ml of 1 X TAE buffer (40mM Tris and 1mM EDTA) with Ethidium Bromide (EtBr) incorporated. DNA was observed from the gels under UV illumination.

Sequencing of PCR products. The PCR products were purified using the MinElute PCR purification kit (Qiagen, Germantown, MD) as follows: Five volumes (200 µl) of buffer PB were added to each PCR reaction (40 µl) sample tube and mixed by pipetting and centrifuged for 1 minute at 13,000 rpm in a MinElute column. Flow-through was discarded and the column was centrifuged for an additional 1 minute at 13,000 rpm. The column was placed into a new 1.5 ml microcentrifuge tube and 10 µl of elution buffer EB was added to the center of the column membrane. After 1 minute the columns were centrifuged again at 13, 000 rpm to collect eluted PCR product.

Twenty nanograms of DNA template was calculated from each sample based on DNA concentration measurements using an Eppendorf Biophotometer 6131. To the DNA template was added 1 µl of primer ITS1 or ITS4 (2 µM) and the total volume to 6.5 µl was obtained by adding molecular grade water.

Sequence analysis and BLAST search. Sanger sequencing was done by the Nevada Genomics Center (Reno, NV). Forward and reverse sequences from PCR amplicons were assembled and compared to sequences deposited in

the NCBI (National Center for Biotechnology Information) using BLAST (Basic Local Alignment Search Tool) (Altschul *et al*., 1990). DNASTAR MegAlign Pro Ver. 15.3.0.66 was used to compare species.

RESULTS

Fungal isolates associated with symptomatic plants and their colony characteristics. Fungal colonies formed within five days after plating. Of the 85 plated root tissue pieces, 67 tissue pieces grew distinct fungal colonies. From these, thirty-four representative fungal colonies were transferred to fresh PDA media for further observations. The thirty-four fungal isolates were grouped into 6 types based on initial colony characteristics (Fig. 1-2). Colony type one contained 14 isolates and was white in color. Colony type two contained 5 isolates and was white to light beige in color. Colony type three contained 1 isolate and was white in color and less compact. Colony type four contained 3 isolates, was pink in color, and grew dense and slowly. Colony type five contained 5 isolates, had fluffy grey to white aerial mycelia, and grew quickly. Colony type six contained 2 isolates and was green in color.

Amplification of the ITS region of rDNA. DNA was extracted from the 34 fungal isolates with concentrations ranging from 2.5 to 201.7 ng/µl. The ITS region of rDNA was successfully amplified from all 34 isolates. All amplicons were approximately 500-550 bp in size (Fig. 1-3). Isolates R11 and R13, which were apparently different from *Fusarium* genus morphologically, had two amplicons and their PCR products were not purified or processed further for sequencing. The PCR products of the remaining thirty-two isolates were purified and processed for sequencing as described.

Species identification. The purified PCR products of 32 fungal isolates were successfully sequenced. Based on BLAST searches, 28 of the isolates were *Fusarium* species, two isolates were *Ascomycota sp.*, and two isolates were *Trichoderma* sp. From the sequencing data, *Fusarium* isolates were identified as *F. oxysporum* (544bp), *F. solani* (566 bp), *F. redolens* (559 bp), *F. tricinctum* (536 bp), and *F. equiseti* (546 bp), consistent with initial colony grouping (Table 1-1). Of the 28 isolates identified as belonging to the genus *Fusarium*, their ITS regions of DNA sequences were 99% or higher identical to the same region of *F. oxysporum* (GenBank accession no. MN153518), *F. solani* (GenBank accession no. KK617035), *F. equiseti* type specimen (GenBank accession no. NR_121457) (O'Donnell *et al.*,2009), *F. tricinctum* type specimen (GenBank accession no. MH862424) (Vu *et al*., 2019), and *F. redolens* (GenBank accession no. MT563396). Aligning the consensus sequences obtained from these 5 species suggested that there are significant sequence differences in the ITS region of rDNA among these species (Fig. 1-4).

DISCUSSION

In this study, we used the ITS region of rDNA amplified by the ITS1/ITS4 primer pair to identify the fungal species isolated from symptomatic hemp plants and found that five *Fusarium* species were associated with severe root rot and sudden death of an industrial hemp crop. Of the five *Fusarium* species detected, *F. oxysporum* was the most prevalent species that was isolated from 82% of the plated tissue pieces, *F. solani*, *F. equiseti*, *F. tricinctum*, and *F. redolens* were isolated from 29%, 29%, 18%, and 6% of sampled plants, respectively.

Trichoderma virens, an antagonist to *Fusarium* was also isolated from diseased root tissue. *Trichoderma* species are natural bio-control agents and have been used in agricultural applications to protect plant health (Harman, 2006). The positive isolation of *Trichoderma virens* suggests that the root-rot disease can be potentially suppressed by this *Trichoderma* species if introduced. It is not surprising that two Ascomycota fungi were also isolated from diseased roots. However, these two unidentified fungal species (sequence data are inconclusive) were only recovered from diseased root tissue with very low frequency and without direct evidence of their link to the disease symptoms.

While GenBank is a particularly useful source for the identification of plant pathogens, it may contain some misidentified and uncurated sequences (Bidartondo *et al*., 2008). To ensure more accurate identifications, sequence data from type materials or voucher specimens should be used if available. Type material is the taxonomic reference from which physical specimens are initially

identified and named, and sequences from these type specimens are a high-value subset of GenBank for which we can maintain a high level of confidence in the taxonomic identification (Federhen, 2015). A voucher specimen is a representative sample of an expertly identified organism that is deposited and stored at a facility from which researchers may later obtain the specimen for examination and further study. Vouchers are vital for the authentication of the taxonomy of an organism (Culley, 2013). Our sequence data matched either type or voucher specimen sequences which provided a high level of confidence in species determination. Additional loci may be used, if necessary, for further confirmation. For example, translation elongation factor 1-α (TEF1) and DNA directed RNA polymerase II largest subunit (RPB1) and second largest subunit (RPB2) are often used in species identification (Lutzoni *et al*., 2004; James *et al*., 2006).

The five *Fusarium* species isolated and identified from infected roots in this study are speculated to be the major cause of root rot disease as many *Fusarium* species, especially *F. oxysporum* and *F. solani* are well established in causing root rots and wilts on a wide range of plant species (Leslie & Summerell, 2006; Argios, 1997). The data obtained in this study suggest that *F. oxysporum*, *F. solani*, and *F. redolens* are likely the primary pathogens, while *F. tricinctum* and *F. equiseti* may be secondary pathogens. However, the role of each species in the disease development remains to be investigated, especially for *F. tricinctum*, *F. redolens*, and *F. equiseti*.

The scale of plants killed, extent of root rot, and co-infections by multiple *Fusarium* species imply that hemp is very susceptible to infection by *Fusarium* species, including some of those considered as weak or secondary pathogens. This may be due to the lack of resistant mechanisms in *Cannabis* plants. However, it is not known if other organisms were involved in this disease, causing hemp plants to be more susceptible to *Fusarium* infection. In fact, *Fusarium* root rots are sometimes associated with other injuries, environmental stress, or nematode infections (Di Pietro *et al*., 2003). Since the disease occurred in arid conditions during the summer, the environmental stress, mainly drought may have played a role in the disease development (Argios, 1997).

Table 1-1. Initial Fungal isolate characteristics and species identification.

Fungal isolate	Colony color	PCR amplicon size (bp)	BLAST suggested identity	Accession number	Identity rate (%)
R1	White	544	*Fusarium oxysporum*	MN153518	100.0
R4	White	544	*Fusarium oxysporum*	MN153518	100.0
R5	White	544	*Fusarium oxysporum*	MN153518	100.0
R6	White	544	*Fusarium oxysporum*	MN153518	100.0
R8	White	544	*Fusarium oxysporum*	MN153518	100.0
R9	White	544	*Fusarium oxysporum*	MN153518	100.0
R12	White	544	*Fusarium oxysporum*	MN153518	100.0
R14	White	544	*Fusarium oxysporum*	MN153518	100.0
R15	White	544	*Fusarium oxysporum*	MN153518	100.0
R16	White	544	*Fusarium oxysporum*	MN153518	100.0
R17	White	544	*Fusarium oxysporum*	MN153518	100.0
R18	White	544	*Fusarium oxysporum*	MN153518	100.0
R19	White	544	*Fusarium oxysporum*	MN153518	100.0
R21	White	544	*Fusarium oxysporum*	MN153518	100.0
R2	White to beige	566	*Fusarium solani*	KY617035	100.0
R20	White to beige	566	*Fusarium solani*	KY617035	100.0
R27	White to beige	566	*Fusarium solani*	KY617035	100.0
R29	White to beige	566	*Fusarium solani*	KY617035	100.0
R30	White to beige	566	*Fusarium solani*	KY617035	100.0
R3	White	559	*Fusarium redolens*	MT563396	100.0
R22	Pink	563	*Fusarium tricinctum*	MK790114	100.0
R23	Pink	563	*Fusarium tricinctum*	MK790114	100.0
R25	Pink	563	*Fusarium tricinctum*	MK790114	100.0
R7	Grey to white	546	*Fusarium equiseti*	MK621018	100.0
R10	Grey to white	546	*Fusarium equiseti*	MK621018	100.0
R28	Grey to white	546	*Fusarium equiseti*	MK621018	100.0
R31	Grey to white	545	*Fusarium equiseti*	MT626672	100.0
R32	Grey to white	545	*Fusarium equiseti*	MT626672	100.0

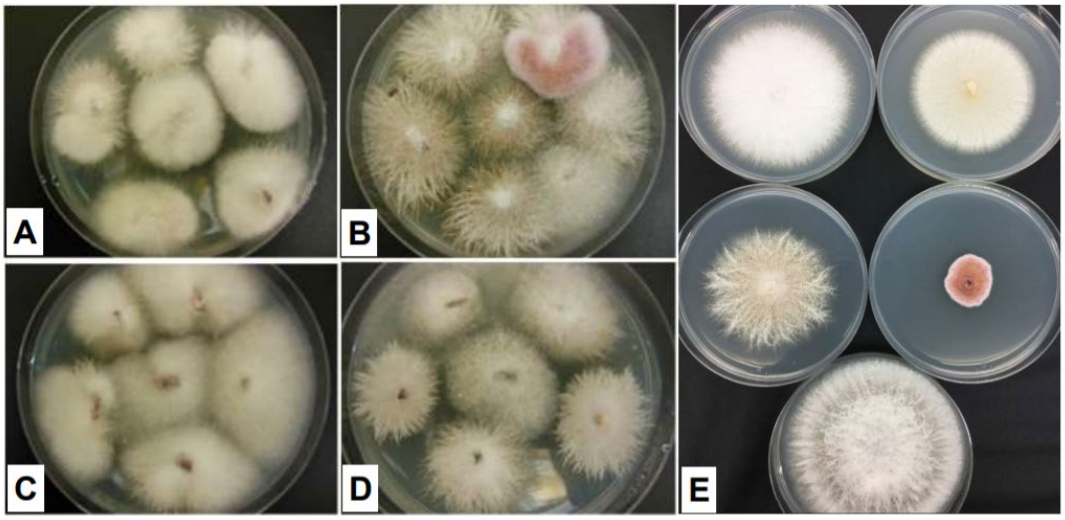

Figure 1-2. *Fusarium* colonies grown from diseased hemp root tissue on PDA+strep. **A.** *Fusarium* colonies from "Canda" hemp variety. **B.** *Fusarium* colonies from "Futura-75" hemp variety. **C.** and **D.** *Fusarium* colonies from Joey hemp variety. **E.** Characteristics of one week old colonies of *F. oxysporum* (upper left), *F. solani* (upper right), *F. redolens* (middle left), *F. tricinctum* (middle right) and *F. equiseti* (bottom) on PDA medium amended with streptomycin sulfate. (Photo by Shouhua Wang)

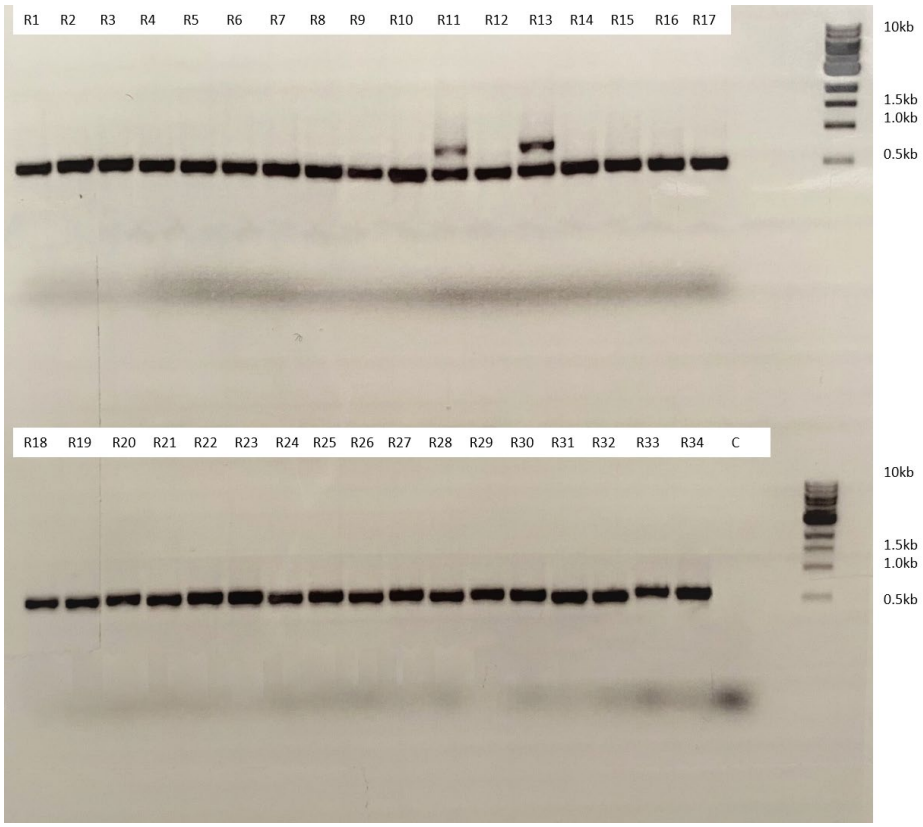

Figure 1-3. PCR amplifications of the ITS region of rDNA of 34 fungal isolates visualized on 1% agarose gel. The primer pair used was ITS1/ITS4. All isolates generated an amplicon of approximately 600 bp. Top lanes: isolates R1 through R17, bottom lanes: isolates R18 through 34, far right well of the bottom row: non-template control. The DNA ladder used was 1 kb (New England Biolabs) and was in the outermost right well of both rows. Isolates R11 and R13 had two amplicons, which might suggest the impurity of these two isolates.

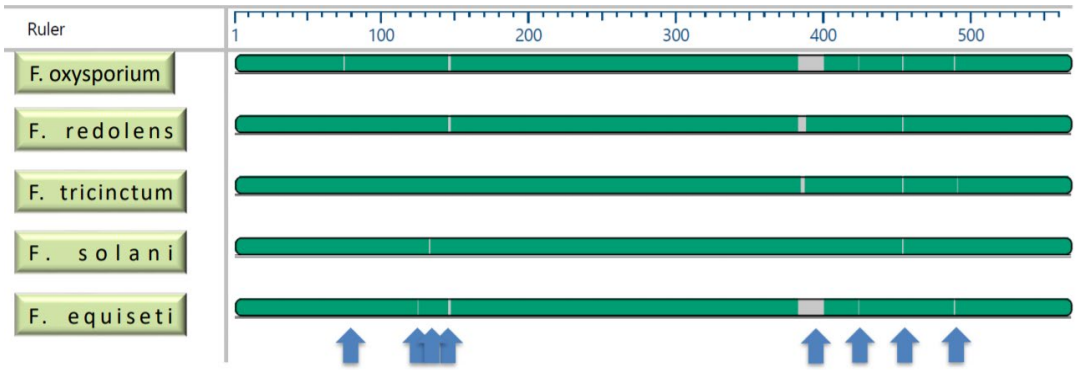

Figure 1-4. Alignment of PCR sequences from 5 *Fusarium* species. Five distinct *Fusarium* species were identified from 28 fungal isolates based on DNA sequences of the ITS region of rDNA obtained through PCR using ITS1/ITS4 primer pair. From the sequencing data, isolates were identified as *F. oxysporum* (544bp), *F. solani* (566 bp), *F. redolens* (559 bp), *F. tricinctum* (536 bp), and *F. equiseti* (546 bp). Consensus sequences from each species were obtained by multi-alignment. The base differences among these five *Fusarium* species are shown as grey and indicated by the arrows at bottom of figure. The identical sequences are indicated as green.

LITERATURE CITED

Altschul, S.F., Gish, W., Miller, W., Myers, E.W. & Lipman, D.J. (1990). Basic local alignment search tool. *Journal Molecular Biology*. 215: 403-410.

Badotti, F., de Oliveira, F.S., Garcia, C.F. Vaz, A.B., Fonseca, P.L., Nahum, L.A., Oliveira, G., & Góes-Neto, A. (2017). Effectiveness of ITS and sub-regions as DNA barcode markers for the identification of Basidiomycota (Fungi). *BMC Microbiology*. 17: 42.

Bellemain E., Carlsen T., Brochmann C., Coissac E., Taberlet P., & Kauserud H. (2010). ITS as an environmental DNA barcode for fungi: an *in silico* approach reveals potential PCR biases. *BMC Microbiology*.10:189.

Bidartondo, M., Bruns, T., Blackwell, M., Edwards, I., Taylor, A., Horton, T., Zhang, N., Kõljalg, U., May, G., Kuyper, T., Bever, J., Gilbert, G. Taylor, J., DeSantis, T., Pringle, A., Borneman, J., Thorn, Greg, R., Berbee, M., Mueller, G., & Ryberg, M. (2008). Preserving accuracy in GenBank. *Science* 319: 1616.

Coleman, J. (2016). The *Fusarium solani* species complex: Ubiquitous pathogens of agricultural importance. *Molecular Plant Pathology. 17*(2),146-58.

Culley T. M. (2013). Why vouchers matter in botanical research. *Applications in Plant Sciences*. *1*(11).

Di Pietro, A., Madrid, M.P., Caracuel, Z., Delgado-Jarana, J. & Roncero, M.I.G. (2003). *Fusarium oxysporum*: exploring the molecular arsenal of a vascular wilt fungus. *Molecular Plant Pathology*. 4: 315–325.

Federhen, S. (2015). Type material in the NCBI taxonomy database. *Nucleic Acids Research*, 43: 1086–1098.

Goswami, R.S. & Kistler, H.C. (2004). Heading for disaster: *Fusarium graminearum* on cereal crops. *Molecular Plant Pathology*. 5: 515–525.

Harman, G.E. (2006). Overview of mechanisms and uses of *Trichoderma* spp. *Phytopathology*. 96: 190–194.

James, T.Y., Kauff, F., Schoch, C.L., Matheny, P.B., Hofstetter, V. Cox, C.J., Celio, G., Gueidan, C., Fraker, E., Miadlikowska, J., Lumbsch, H.T., Rauhut, A., Reeb, V., Arnold, A.E., Vilgalysmtoft, A.R., Stajich, J.E., Hosaka, K., Sung,

G.H., Johnson, D., … O'Rourke, B. (2006). Reconstructing the early evolution of Fungi using a six-gene phylogeny. *Nature*. 443: 818–822.

Leslie, J.F & Summerell, B.A. (2006). *The Fusarium Laboratory Manual.* Blackwell Publishing, USA.

Lutzoni, F., Kauff, F., Cox, C. J., McLaughlin, D., Celio, G., Dentinger, B., Padamsee, M., Hibbett, D., James, T. Y., Baloch, E., Grube, M., Reeb, V., Hofstetter, V., Schoch, C., Arnold, A. E., Miadlikowska, J., Spatafora, J., Johnson, D., Hambleton, S., Crockett, M., … Vilgalys, R. (2004). Assembling the fungal tree of life: progress, classification, and evolution of subcellular traits. *American journal of botany*, *91*(10), 1446–1480.

O'Donnell, K., Sutton, D.A., Rinaldi, M.G., Gueidan, C., Crous, P.W. & Geiser, D.M. (2009). Novel multilocus sequence typing scheme reveals high genetic diversity of human pathogenic members of the *Fusarium incarnatum-F. equiseti* and *F. chlamydosporum* species complexes within the United States. *Journal of Clinical Microbiology*. *47* (12), 3851-3861.

Schoch, C.L., Seifert, K.A., Huhndorf, S., Robert, V., Spouge, J.L., Levesque, C.A., & Chen, W. (2012). Fungal barcoding consortium. Nuclear ribosomal internal transcribed spacer (ITS) region as a universal DNA barcode marker for fungi. *PNAS. 109* (16), 6241–6246.

Vu, D., Groenewald, M., de Vries, M., Gehrmann, T., Stielow, B., Eberhardt, U., Al-Hatmi, A., Groenewald, J.Z., Cardinali, G., Houbraken, J., Boekhout, T., Crous, P.W., Robert, V. & Verkley, G.J.M. (2019). Large-scale generation and analysis of filamentous fungal DNA barcodes boosts coverage for kingdom fungi and reveals thresholds for fungal species and higher taxon delimitation. *Studies in Mycology*. 92: 135-154

White, T. J., T. Bruns, S. Lee, & J. W. Taylor. (1990). Amplification and direct sequencing of fungal ribosomal RNA genes for phylogenetics. Pg. 315-322 In: *PCR Protocols: A Guide to Methods and Applications*, eds. Innis, M. A., D. H. Gelfand, J. J. Sninsky, and T. J. White. Academic Press, Inc., New York.

Chapter Two:

The molecular identification of a *Golovinomyces* species causing powdery mildew on *Cannabis sativa* plants based on the ITS region of rDNA.

ABSTRACT

Cannabis plants (*Cannabis sativa* L.) are cultivated in registered indoor facilities in Nevada. Powdery mildew is one of the most common diseases in indoor cultivation facilities, but it is not completely known what specific fungal species are associated with cannabis plants. In 2017, a powdery mildew infection was observed on most cannabis plants in an indoor cultivation facility. Infected leaves were placed under a dissecting microscope and mycelium and spores were blotted onto a piece of clear tape and mounted on a slide for morphological examination. Sequencing of the ITS regions of rDNA from the spores led to the identification of this fungus as *Golovinomyces ambrosiae*. To our knowledge, this is the first report of this species infecting *C. sativa* in Nevada.

INTRODUCTION

Cannabis sativa is an herbaceous flowering plant in the family *Cannabaceae*. This regulated cannabis species is grown in indoor cultivation facilities. Infectious plant diseases of indoor-grown cannabis may occur during cultivation, and a year-round growing season may generate significant disease pressure for plants. Information on diseases of *Cannabis* species is still limited and accurate identification of pathogens impacting this crop is critical for disease mitigation.

Powdery mildew fungi are a group of widespread, well-known obligate fungal parasites that negatively impact a diverse array of host plants in a variety of environmental conditions (Ale-Agha *et al.*, 2008). Conditions in indoor growing facilities are often favorable for powdery mildews, which promotes spore germination, dissemination, and repeated infection (Gubler, 1999). Powdery mildew infections can impair photosynthesis which may lead to decreased growth and early senescence. Powdery mildews can result in severe crop losses if left untreated. As powdery mildew fungi cannot be cultured as they are obligate parasites, molecular methods are often used for species identification and genus groupings (Braun *et al.*, 2002).

Recently, powdery mildew caused by *Golovinomyces ambrosiae* was reported on industrial hemp in Oregon (Wiseman *et al*., 2021). In 2019 Powdery mildew caused by *Golovinomyces spadiceus* was reported from cannabis plants in indoor facilities in Canada (Punja *et al*., 2019). In 2018, powdery mildew

caused by *Golovinomyces cichoracearum sensu lato* was reported on cannabis in Canada (Pépin *et al.*, 2018). In 2017, we detected a powdery mildew infection from an indoor growing facility in Carson City County. Infected plants were submitted to our lab by cultivators and had dense clusters of white spores and mycelia growing on the upper leaf surfaces. Here we report a powdery mildew disease on cannabis plants caused by *Golovinomyces ambrosiae* based on the ITS region of rDNA.

MATERIALS AND METHODS

Observation of symptomatic leaf samples. Leaflets with patches of white, powdery growth on leaf surfaces were submitted to the lab by a cultivator. The leaflets were initially observed under a dissecting microscope to determine the nature of the white, powdery material. A powdery mildew fungus was confirmed by its morphological characteristics.

Spore collection for DNA extraction or direct PCR. The areas surrounding the dissecting microscope were disinfected with 70% ethanol (EtOH) prior to spore collection from the sample. All tools used were disinfected by submerging in 70% EtOH and flame sterilization. Under the dissecting microscope, patches of powdery mildew were located, and 15 µl of IDTE (10 mM Tris, 0.1 mM EDTA) suspension buffer was pipetted several times on the surface of the powdery mildew to collect spores and mycelia into a 0.2 ml PCR tube. Five microliters of this spore suspension were transferred to a new PCR tube in which 9 µl of sterile water was added. The resulting solution was mixed and spun down as one sample. A total of 8 spore samples were taken as described from different powdery mildew patches, respectively. For comparison, half of the samples (samples 5-8) were proceeded to DNA extraction using Plant DNeasy kits (Qiagen) to obtain genomic DNA prior to the PCR, the remaining samples (samples 1-4) were heated at 100°C for 10 minutes and then proceeded to PCR directly without DNA extraction steps – direct colony PCR.

PCR amplification of the ITS region of rDNA. Both spore preparation and purified DNA were used for PCR. The primer pair ITS1 (5'-TCCGTAGGTGAACCTGCGG-3') and ITS4 (5'-TCCTCCGCTTATTGATATGC-3') (White *et al.*, 1990) were used to amplify the ITS region of rDNA. The PCR procedure was performed as described in Chapter One. PCR products were electrophoresed on a 1% agarose gel as described in Chapter One.

DNA sequencing of PCR products. PCR products were purified and prepared for Sanger sequencing as described in Chapter One.

Sequence analysis and species identification. Sequence analysis was performed as described in Chapter One. Assembled sequences were subjected to BLAST searches to find closely related species.

RESULTS

Amplification of the ITS region of rDNA. Following DNA extraction with Qiagen Plant DNeasy, the DNA concentrations for 4 samples were 10.0 ng/µl, 2.5 ng/µl, 2.5 ng/µl, and 10.0 ng/µl, respectively. The other 4 samples were not processed for DNA extraction and were directly proceeded to PCR after heating at 100°C for 10 minutes. Following PCR, all 8 samples generated sufficient amplicons with DNA concentrations of 56.0 ng/µl, 58.6 ng/µl, 73.3 ng/µl, 62.3 ng/µl, 61.3 ng/µl, 58.6 ng/µl, 62.4 ng/µl, and 26.5 ng/µl, respectively. There was no significant difference between the PCR directly from spore samples and the PCR from purified DNA samples. All amplicons were approximately 600 bp (Fig. 2-1). PCR products amplified directly from spores without DNA extraction appear to have robust amplification (strong bands), while PCR amplifications from purified DNA appeared to be weak. Although all PCR products were measured to be of similar concentrations by the photometer reading, the gel revealed the direct PCR was a more sensitive and quick method to detect the fungal DNA. The first 5 PCR reactions (as shown in Fig. 2-1) were purified and submitted for Sanger sequencing.

Species identification. All five DNA samples were successfully sequenced and assembled to obtain full amplicon sequences. All 5 samples had a 596 bp amplicon and were identical (Fig. 2-2). BLAST searches confirmed that the sequence data obtained from this fungus are identical to that of voucher

specimen of *Golovinomyces ambrosiae* (GenBank accession no. KM657962) (Cho *et al*., 2011), and this supports our identification of this fungus as *Golovinomyces ambrosiae.*

DISCUSSION

This study confirmed that the causative agent of a powdery mildew outbreak in a medical cannabis facility in Nevada was *G. ambrosiae* based on ITS rDNA region sequences. This pathogen has not been previously reported on *C. sativa* in Nevada.

While BLAST searches generated many hits to *Golovinomyces* species, many of those sequences were not based on the vouchered specimen. The PCR amplicon sequence obtained from the cannabis powdery mildew fungus completely matches that of the *Golovinomyces ambrosiae* voucher specimen, which gave us the highest confidence in this determination.

The method of direct PCR from spore masses was confirmed to be a quick method to amplify fungal DNA without performing a DNA extraction procedure. Because obligate pathogens like powdery mildew fungi are not culturable and difficult to generate enough mass for DNA extraction, direct PCR from a small number of spores is an alternative. In this case, DNA extracted from limited spores might cause loss of template and therefore resulted in poor amplification while compared to the direct PCR that yielded strong bands (Fig. 2-1).

Resolution within taxonomy based on only ITS sequences may be insufficient to discriminate closely related powdery mildew species (Takamatsu *et al*., 2013). Multi locus analyses may be used to further distinguish some species in closely related complexes (Qiu *et al*., 2020). In this study, the powdery mildew

fungus identified from cannabis was confirmed to be *G. ambrosiae* based on the ITS rDNA sequences.

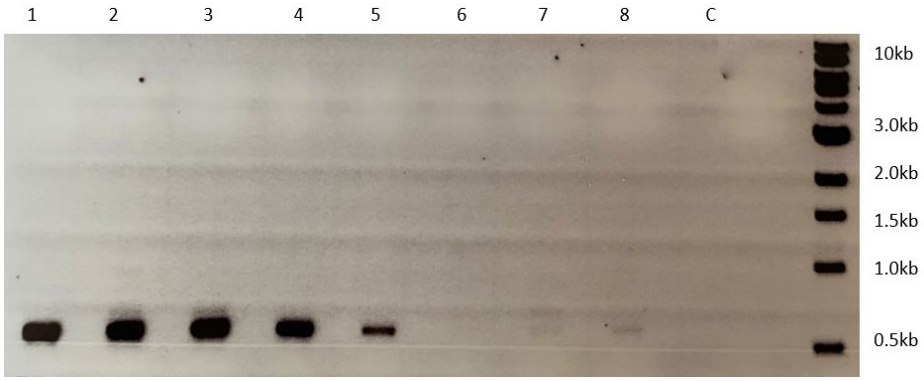

Figure 2-1. Gel electrophoresis showing amplification of the ITS region of rDNA of 8 powdery mildew fungal samples. Lanes 1-4: PCR amplification directly from collected spores after heating. Lanes 5-8: PCR amplification from the DNA extracted from spores. Lane “C”: non-template control (molecular grade water). Far right lane: DNA ladder (1 kb, New England Biolabs).

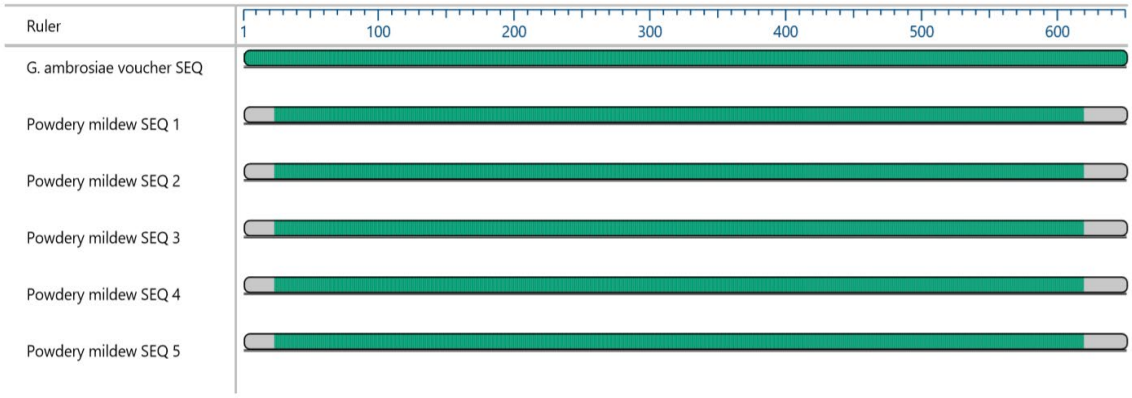

Figure 2-2. Multi-alignment of PCR amplicons (ITS region of rDNA) generated from 5 powdery mildew fungal samples with the corresponding region of a vouchered *Golovinomyces ambrosiae* specimen (KM657962). All five sequences were 100% identical to that of a *G. ambrosiae* voucher specimen (Cho *et al*., 2011).

LITERATURE CITED

Ale-Agha, N., Boyle, H., Braun, U., Butin, H., Jage, H., Kummer, V. & Shin, H.D. (2008). Taxonomy, host range and distribution of some powdery mildew fungi (Erysiphales). *Schlechtendalia* 17: 39–54.

Braun, U., Cook, R.T.A., Inman, A.J. & Shin, H.D. (2002). The Taxonomy of the Powdery Mildew Fungi. Pages 13-55 in: *The Powdery Mildews: a Comprehensive Treatise,* Berlanger, R.R., W.R. Bushnell, A.J. Dik, and T.L.W Carver (eds.). American Phytopathological Society, St Paul.

Cho, S. E., Park, J. H., Park, M. J., & Shin, H. D. (2011). First report of powdery mildew caused by *Golovinomyces ambrosiae* on *Ambrosia trifida* in Korea. *Plant Disease. 95* (11), 1480-1480.

Gubler, W.D., Rademacher, M.R. & Vasquez, S.J. (1999). Control of powdery mildew using the UC Davis powdery mildew risk index. APSnet Features.

Pépin, N., Punja, Z. K., & Joly, D. L. (2018). Occurrence of powdery mildew caused by *Golovinomyces cichoracearum* sensu lato on *Cannabis sativa* in Canada. *Plant Disease*. 102: 1226.

Punja, Z.K., Collyer, D., Scott, D., Lung, S., Holmes, J. & Sutton, D., (2020). Pathogens and molds affecting production and quality of *Cannabis Sativa* L. *Frontiers in Plant Science*. 10: 1120.

Qiu, P.-L., Liu, S.-Y., Bradshaw, M., Rooney-Latham, S., Takamatsu, S., Bulgakov, T. S., … Braun, U. (2020). Multi-locus phylogeny and taxonomy of an unresolved, heterogeneous species complex within the genus Golovinomyces (Ascomycota, Erysiphales), including G. ambrosiae, G. circumfusus and G. spadiceus. *BMC Microbiology*, *20*(1). doi:10.1186/s12866-020-01731-9

Takamatsu, S., Matsuda, S., & Grigaliūnaitė, B. (2013). Comprehensive phylogenetic analysis of the genus *Golovinomyces* (Ascomycota: Erysiphales) reveals close evolutionary relationships with its host plants. *Mycologia*.105:1135–52.

White, T. J., T. Bruns, S. Lee, & J. W. Taylor. (1990). Amplification and direct sequencing of fungal ribosomal RNA genes for phylogenetics. Pp. 315-322 In: *PCR Protocols: A Guide to Methods and Applications*, eds. Innis, M. A., D. H. Gelfand, J. J. Sninsky, and T. J. White. Academic Press, Inc., New York.

Wiseman, M.S., Bates, T., Garfinkel, A., Ocamb, C.M., & Gent, D.H. (2021). First report of powdery mildew caused by *Golovinomyces ambrosiae* on *Cannabis sativa* in Oregon. *Plant Disease*. Epub ahead of print.

Chapter Three:

The molecular identification of *Alternaria* species associated with imported hemp seeds through the ITS region of rDNA.

ABSTRACT

Industrial hemp (*Cannabis sativa* L.) is an emerging crop in Nevada. Industrial hemp seeds used for crop cultivation are either imported from foreign countries or produced domestically. In a germination test conducted on imported hemp seeds, a high rate of fungal growth was observed, suggesting a presence of seedborne fungal organisms. Surface-sterilized seeds were plated on potato dextrose agar amended with streptomycin. While 86% of the plated seeds germinated, 56% of the plated seeds had fungal growth, the majority of which had fungal colonies grown from newly germinated tap roots. A total of 29 *Alternaria* isolates were obtained and maintained for morphological observations. One visually distinct type contained 14 isolates with white to gray colonies and another had 15 isolates with gray to black colonies. DNA was extracted from all isolates and PCR was performed using primers ITS1/ITS4 to amplify the ITS region of rDNA. The size of PCR amplicons obtained from the 24 isolates ranged from 542 to 600 bp. A BLAST search suggested that these two types of isolates were closely related to *Alternaria infectoria* and *A. tenuissima*, respectively. The data suggest that hemp seeds of the “Canda” variety carried two distinct *Alternaria* species, but the effects of these two fungal species on the health of seeds or seedlings are not known.

INTRODUCTION

Plant diseases associated with hemp crops have been occurring in Nevada in recent years. Information on diseases of *Cannabis* species is still limited and growers often lack management strategies to cope with sudden outbreaks of infectious diseases. While more diseases are being found in the field, it is not known how hemp seeds may be playing a role in the pathway of diseases associated with industrial hemp. There is a possibility that imported, or domestically produced hemp seeds may carry certain pathogens that can cause an outbreak of disease following planting or germination.

Most *Alternaria* species are mainly saprophytic, but some species also function as pathogens causing diseases of cultivated plants (Thomma, 2003). *Alternaria* is ubiquitous and associated with a wide variety of substrates including seeds. When conditions are favorable, certain species can cause serious diseases and crop loss. In some crops, seeds are a major means to carry *Alternaria* to the subsequent crop (Woudenberg *et al*., 2013).

The genus *Alternaria* contains over 50 pathogenic and non-pathogenic species, some of which may be morphologically similar or do not produce characteristic spores. Identification of an unknown isolate to the species by morphological methodology is time-consuming, requires a familiarity with specific fungal morphology, and in many cases, may not be accurate (Arzanlou *et al*., 2007; Loganathan *et al*., 2016). The use of DNA-based identifications using certain genetic loci makes the organism identification process much quicker. The

most commonly used locus for species identification in fungi is the internal transcribed spacer region of ribosomal DNA (ITS rDNA) (Mohammadi & Bahramikia, 2019).

To verify germination rates of imported hemp seeds (variety ‘Canda’), selected seeds were placed on dampened germination paper and incubated at 20°C under 16 hours of lighting. Many of the seeds, when germinated, were covered by dense fungal mycelia that normally do not appear in germination trials with healthy seeds. To characterize and identify the fungal species associated with these imported hemp seeds, both morphological and molecular approaches were employed. In this chapter, we present our findings that two distinct *Alternaria* species were carried by hemp seeds based on both their morphological characteristics and DNA sequences at the ITS region of rDNA.

MATERIALS AND METHODS

Seed germination test and fungal growth observations. Two hundred seeds were placed on heat-sterilized filter paper that was moistened with sterile water in a germination tray and incubated in a germinator at 20°C with 16 hours of lighting. Germination and potential fungal growth from seeds were monitored daily until most or all seeds had germinated. Germination trays with fungal growth were further examined under stereo and compound microscopes to preliminarily identify the type of fungi for further study.

Fungal isolation from seeds. Inside a biosafety cabinet, fifty seeds were surface sterilized by shaking in a 50 ml falcon tube with 20 ml of 1% sodium hypochlorite (NaOCl) solution for 15 minutes, followed by rinsing three times in sterilized water. Seeds were then placed onto sterilized filter paper to blot dry and plated onto potato dextrose agar amended with streptomycin sulfate (PDA+streptomycin) with 3 seeds per plate. Plates were incubated at 22°C in the dark. Within a week, representative fungal colonies were transferred to new PDA plates and maintained on PDA slants for morphological studies.

DNA extraction from fungal mycelium. Mycelia from each isolate were collected from the colony on the PDA plate using a sterilized scalpel. Approximately 200 mg of mycelia with spores was collected in a sterile 1.5 ml LysingMatrixA tube and then proceeded to DNA extraction using a Plant DNeasy kit (Qiagen, Germantown, MD) following procedures as described in Chapter One.

PCR amplification of the ITS region of rDNA. Primer pair ITS1 (5'-TCCGTAGGTGAACCTGCGG-3') and ITS4 (5'-TCCTCCGCTTATTGATATGC-3') (White *et al.*, 1990) were used to amplify the ITS regions of rDNA from all isolates using the same procedures as described in Chapter One. Amplification was examined by electrophoresis on a 1% agarose gel and then observed under UV light.

Sanger sequencing of PCR amplicons. PCR products from all isolates were purified and then prepared for Sanger sequencing using the same procedures as described in Chapter One.

Sequence analysis and species identification. Sequences of all isolates were manually assembled to obtain the full amplicon sequences using the procedures described in Chapter One. The final sequences were used as query sequences to search for closely related species in the GenBank database.

RESULTS

Fungi associated with seed germination. In the germination trays, while the majority of seeds germinated, the tray was fully covered with brownish to dark mycelia growing out from many germinated and ungerminated seeds (Fig. 3-1). Fungal mycelia grew along the surface of germination paper, making brown to dark patches in germination trays. The dark patches were confirmed to be the colonies of *Alternaria* fungi by their characteristic thick and dark hyphae and spores.

Fungi isolated from seeds and their colony characteristics. Of the 50 plated seeds, 86% of seeds germinated and 56% of seeds had fungal growth. Noticeably, the majority of infected seeds had fungal colonies growing directly from newly germinated tap roots instead of seed coats. A total of 31 isolates were obtained, 29 were classified as *Alternaria* genus, and 2 as other types of fungi. Among *Alternaria* isolates, 14 had grey to dark grey colonies and 15 had white to grey colonies (Fig. 3-1).

DNA extraction and amplification of the ITS region of rDNA. Genomic DNA of 29 *Alternaria* isolates was extracted followed by PCR using the ITS1/ITS4 primers. The size of the amplicons from all 29 isolates ranged from 542-600 bp (Fig. 3-2 and Table 3-1). One isolate (sample 6) had weak amplification and was not processed for sequencing.

Species identification. Of 29 *Alternaria* isolates, 24 had full amplicon sequences assembled from sequencing data. Five isolates (3, 11, 14, 15, and

25) failed in sequencing. The 24 assembled sequences ranged from 542 to 600 bp (Table 3-2). BLAST searches confirmed that these 24 isolates contain two distinct *Alternaria* species: *Alternaria infectoria* and *A. tenuissima*. Thirteen of the isolates were *A. tenuissima,* of which 11 had 100% identical sequence to that of *A. tenuissima* [GenBank accession nos. MF405157 (2 isolates), MN822571(6 isolates) or MG731240 (3 isolates)], and 2 of which had greater than 99% sequence similarity to MN822571. Eleven of the isolates were identified as *A. infectoria*, with two being 100% identical to GenBank accession nos. MK562061 and KR094467, and 9 isolates were greater than 99% identical to GenBank accession nos. MK562061, KR094467, and KR094465 (Table 3-2). Additionally, 9 of the isolates had greater than 99% sequence similarity to that of type specimen of *A. infectoria* (GenBank accession no. AY751458) and the remaining 2 isolates of *A. infectoria* had greater than 98% identical sequence to that of the same type specimen.

DISCUSSION

In this study, we used both morphological and molecular methods to characterize fungi associated with hemp seeds and confirmed that imported industrial hemp seeds (Var. “Canda”) were infected with two distinct species of *Alternaria: Alternaria tenuissima* and A. *infectoria.* This is an important finding as both species can serve as opportunistic pathogens. *Alternaria* fungi are widely distributed and capable of infecting a broad range of plant species (Simmons, 2007). The detection of *Alternaria* species from hemp seeds suggests that these fungi can successfully infect seed tissue without visible damage to seed integrity and can be latent during the life of seeds.

DNA sequences in the ITS region of rDNA are considered sufficient for genus and species level identification (Pastor & Guarro, 2008). However, it is estimated that more than 14% of GenBank sequences of *Alternaria* species have been misclassified; therefore, unknown sequences should be compared to those of well-characterized reference organisms whenever possible to make more reliable identifications (Woudenberg *et al.,* 2013). The ITS region of rDNA sequences for *A. tenuissima* isolates did not hit sequences of a voucher specimen, but all matched *A. tenuissima* sequences in GenBank. All *A. infectoria* isolates matched the sequence of a type specimen of *A. infectoria* with greater than 98% identical sequence matching.

Detection of *A. infectoria* and *A. tenuissima* from imported hemp seeds may provide important information on the pathway of *Alternaria* disease.

However, the impact of these seed-carried fungi on the health of hemp crops is unknown and worth further investigations.

Table 3-1. Grouping of *Alternaria* isolates based on colony morphology and ITS region sequences.

Fungal Isolate	Colony Color	PCR amplicon size (bp)	BLAST suggested species	Related accession number	Sequence identity (%)
1	White to gray	599	*Alternaria infectoria*	KR094465	99.83
2	White to gray	600	*Alternaria infectoria*	MK562061	99.83
10	White to gray	600	*Alternaria infectoria*	MK562061	99.83
12	White to gray	600	*Alternaria infectoria*	MK562061	99.83
19	White to gray	576	*Alternaria infectoria*	MK562061	99.64
21	White to gray	600	*Alternaria infectoria*	MK562061	99.83
26	White to gray	600	*Alternaria infectoria*	MK562061	99.83
28	White to gray	600	*Alternaria infectoria*	MK562061	99.83
29	White to gray	574	*Alternaria infectoria*	MK562061	100.00
8	Gray to black	573	*Alternaria infectoria*	KR094467	100.00
24	Dark gray	600	*Alternaria infectoria*	MK562061	99.83
4	Dark gray	543	*Alternaria tenuissima*	MF405157	100.00
5	Dark gray	570	*Alternaria tenuissima*	MN822571	100.00
7	Dark gray	542	*Alternaria tenuissima*	MG731240	100.00
9	Dark gray	571	*Alternaria tenuissima*	MF405157	100.00
13	Dark gray	570	*Alternaria tenuissima*	MN822571	100.00
16	Dark gray	570	*Alternaria tenuissima*	MN822571	100.00
17	Dark gray	542	*Alternaria tenuissima*	MG731240	100.00
18	Dark gray	542	*Alternaria tenuissima*	MG731240	100.00
20	Dark gray	572	*Alternaria tenuissima*	MN822571	99.65
22	Dark gray	573	*Alternaria tenuissima*	MN822571	99.48
27	Dark gray	570	*Alternaria tenuissima*	MN822571	100.00
30	Dark gray	542	*Alternaria tenuissima*	MG731240	100.00
31	Dark gray	542	*Alternaria tenuissima*	MG731240	100.00

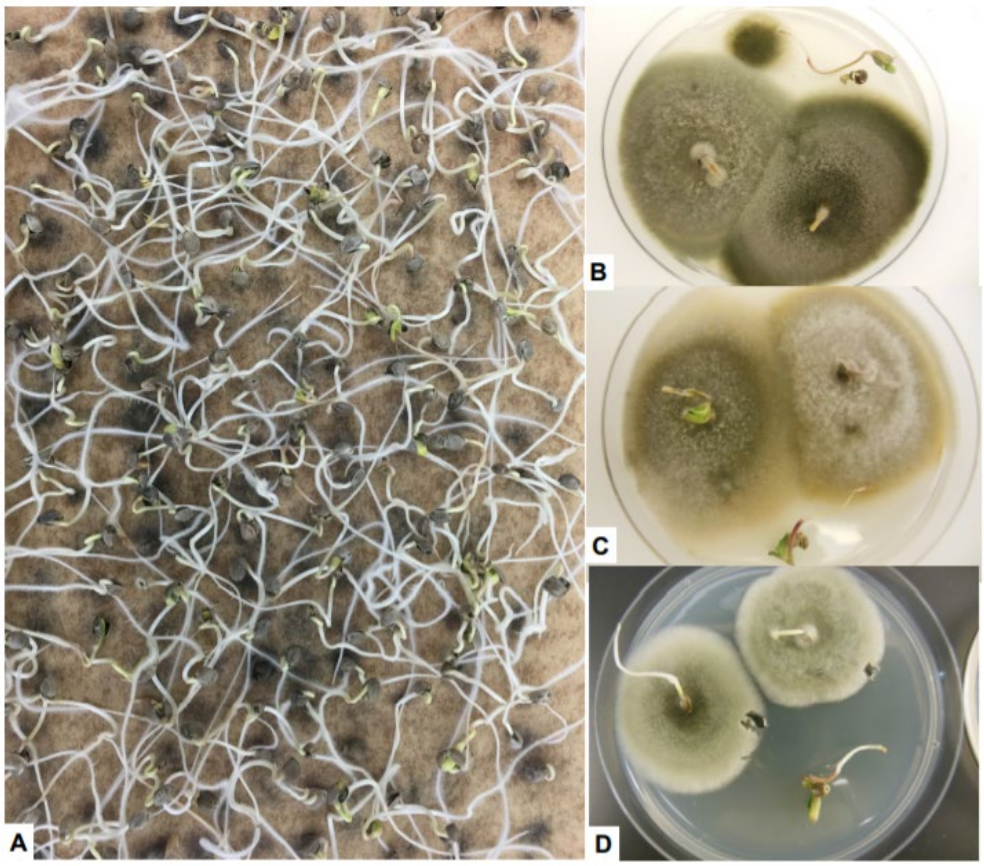

Figure 3-1. Growth of *Alternaria* species from industrial hemp seeds. A. Extensive growth of *Alternaria* mycelia on heat-sterilized filter paper in a germination tray in a growth chamber at 20°C. **B-D.** Colonies of *Alternaria* species grown from individual hemp seeds on PDA plates after seeds were surface sterilized, plated, and incubated in the dark at 22°C. (Photo by Shouhua Wang)

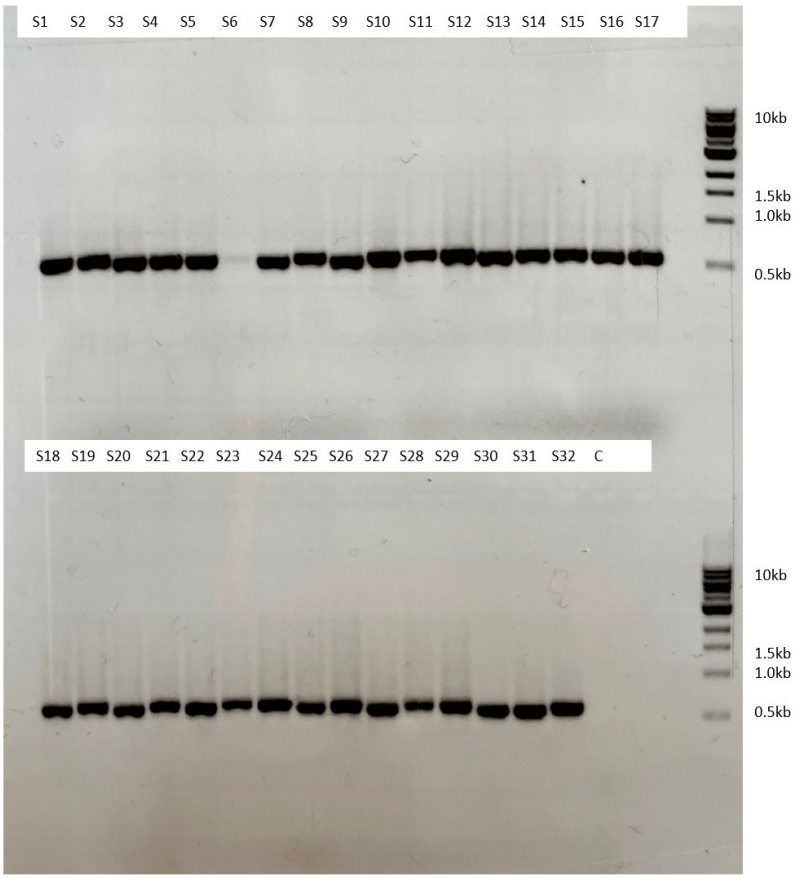

Figure 3-2. PCR amplification of ITS region sequences of 31 fungal isolates from hemp seeds. A single amplicon of 500-600 bp was obtained from each isolate. Top row: samples 1-17, bottom row: samples 18-32. Lane "C": non-template control. The DNA ladder used was 1 kb (New England Biolabs) and is in the outermost right well of each row.

LITERATURE CITED

Arzanlou, M., Abeln, E. C., Kema, G. H., Waalwijk, C., Carlier, J., Vries, I. d., Guzmán, M., & Crous, P. W. (2007). Molecular diagnostics for the sigatoka disease complex of banana. *Phytopathology*, *97*(9), 1112–1118. https://doi.org/10.1094/PHYTO-97-9-1112.

Loganathan, M., Venkataravanappa, V., Saha, S., Rai, A.B., Tripathi, S., Rai, R.K., Tripathi, S., Pandey, A., & Chowdappa, P. (2016). Morphological, pathogenic and molecular characterizations of *Alternaria* species causing early blight of tomato in Northern India. *PNAS. 86*(2), 325-30.

Mohammadi, A., & Bahramikia, S. (2019). Molecular identification and genetic variation of *Alternaria* species isolated from tomatoes using ITS1 sequencing and inter simple sequence repeat methods. *Current Medical Mycology. 5*(2), 1-8.

Pastor, F.J., & Guarro, J. (2008). *Alternaria* infections: laboratory diagnosis and relevant clinical features. *Clinical Microbiology and Infection.14*(8), 734-46.

Simmons, Emory G. (2007). *Alternaria*: *An Identification Manual*. Utrecht, The Netherlands: CBS Fungal Biodiversity Centre. 500–502.

Thomma, B.P.H. J. (2003). *Alternaria* spp.: from general saprophyte to specific parasite. *Molecular Plant Pathology, 4*(4), 226-236.

White, T. J., T. Bruns, S. Lee, & J. W. Taylor. (1990). Amplification and direct sequencing of fungal ribosomal RNA genes for phylogenetics. Pg. 315-322 In: *PCR Protocols: A Guide to Methods and Applications*, eds. Innis, M. A., D. H. Gelfand, J. J. Sninsky, and T. J. White. Academic Press, Inc., New York.

Woudenberg, J.H.C., Groenewald, J.Z., Binder, M., & Crous, P. (2013). *Alternaria* redefined. *Studies in Mycology*. 75: 171-212.

Chapter Four:

The molecular detection of *Beet curly top virus* from hemp based on viral capsid protein gene sequences.

ABSTRACT

In the Fall of 2020, industrial hemp fields located in Douglas, Washoe, and Clark counties in Nevada, exhibited abnormal growth suggesting a virus infection, and either whole plants or affected segments of hemp plants were submitted to our lab for diagnosis. Abnormal leaves displayed distortion, curling at tips, crinkling, vein and petiole reddening, mosaic, and yellowing. Affected plants were underdeveloped. Some plants had symptoms that appeared to be restricted on certain branches, although they were systematically infected. These symptoms suggested an infection by a member of *Curtovirus* such as *Beet curly top virus* (BCTV). To confirm BCTV infection, leaves were collected from fourteen symptomatic hemp plants and two asymptomatic hemp plants. Genomic DNA was extracted from curled leaf tip and swollen petiole tissue of symptomatic plants, and from leaf tips of asymptomatic plants. A PCR assay was performed using general curly top virus primer pair BGv377 and BGc1509. A 1.1 kb DNA fragment was amplified from all symptomatic hemp samples, but not from asymptomatic hemp samples. The PCR products were sequenced and DNA sequences from 5'- and 3'- ends were obtained. Sequence analysis and BLAST search confirmed that the sequences belonged to the part of BCTV capsid protein gene sequence. Assembled 1.1 kb amplicon sequences were greater than 97% identical to GenBank accession nos. KX867042, KX867055, MW188519, and KX867048, which were all from BCTV isolates. To the best of our knowledge, this is the first report of *Beet curly top virus* infecting hemp in Nevada.

INTRODUCTION

Curly top disease in plants is caused by the genus *Curtovirus* belonging to the family *Geminiviridae* with circular ssDNA genomes of approximately 3.0 kb (Chen *et al*., 2010). *Beet curly top virus* (BCTV) is an important member of curtoviruses, causing yield-limiting crop diseases in semiarid production areas of the western United States (Bennett 1971; Strausbaugh *et al*., 2008). BCTV is transmitted among plants by the beet leafhopper, *Circulifer tenellus*, and causes disease in over 300 plant species, including major crops such as sugar beet, tomato, cucurbits, spinach, pepper, and bean (Chen *et al.*, 2010; Bennett, 1971). Typical curly top disease symptoms include inward and upward rolling of leaves, roughening and thickening of leaf veins, leaf dwarfing, vein swelling, leaf crumpling and curling, yellowing, and necrosis of the phloem (Bennett, 1971; Wintermantel, 2009).

In January 2020, BCTV was reported on hemp in Colorado where symptomatic plants exhibited symptoms of leaf yellowing and leaf mosaic (Giladi *et al*., 2020). In December of 2020 BCTV was reported from hemp in Arizona (Hu *et al.,* 2020).

In September of 2020, several plants were submitted to our lab from cultivators in Douglas, Washoe, and Clark counties in Nevada with symptoms characteristic of virus infection. Symptoms varied among plants, but all had leaf distortion, crinkling, curling, mosaic, thickened or swollen veins and petioles, reddening of petioles and veins, and stunted growth (Fig. 4-1). In this chapter we

present the finding of BCTV associated with symptomatic hemp plants in Nevada.

Figure 4-1. Symptoms of hemp plants infected by *Beet curly top virus*. A. Healthy, field-grown hemp plant for comparison to the following observed symptoms: **B.** Leaf curling, crinkling, mosaic, and discoloration (reddening) of midvein and petiole. **C.** Abnormal leaf structure with reddening of midveins, and leaf crinkling. **D.** Pronounced leaf tip curling. **E.** Leaf curling, crinkling, swollen midveins, small leaves. **F.** Swollen midveins, small, abnormal leaves, leaf curling, and reddening of midveins. (Photo by Jennifer Schoener)

MATERIALS AND METHODS

Sample preparation from symptomatic plants. Eleven hemp plants or samples with abnormal growth, leaf yellowing, curling, mosaic, and other symptoms were collected from a field in Douglas county. Two apparently healthy plants were also collected for comparative studies. Three hemp samples suspected of viral infections and submitted by clients from Washoe and Clark counties were also included in this study. All plants and tissue samples were examined for symptoms and a sub-sample of 200 mg each was collected from curled leaf tips and swollen petiole tissue from symptomatic plants or similar tissues from asymptomatic plants for DNA extraction.

Extraction of viral DNA. DNA extraction was performed using Qiagen DNeasy Plant mini kit as described in Chapter One. The extracted DNA was stored at -20°C.

PCR detection of *Beet curly top virus*. The primer pair used for PCR amplification was BGv377 (5'-CTAGCAGTATCGACCAGTTG-3') and BGc1509 (5'-GACATTGACTGGAGACCGTT-3'). These primers amplify a 1.1 kb (*Beet curly top virus*) BCTV capsid protein gene, which includes the entire capsid protein open reading frame (ORF) and parts of the V2, V3, C2, and C3 ORFs. (Soto & Gilbertson, 2003).

The reagents and volumes used for the PCR reaction were as follows per sample: 5 µl of 10X PCR buffer, 1.5 µl of $MgCl_2$ (50 mM), 1 µl of dNTP mixture (10 mM), 2.5 µl BGv377 primer (10 µM), 2.5 µl BGc1509 primer (10 µM), 0.2 µl

Platinum *Taq* polymerase, 36.3 µl of molecular biology grade water, and 1 µl of template DNA. For all samples, PCR was run at 1) original DNA concentrations, 2) at a 1:10 dilution, and 3) at a 1:100 dilution, to optimize the amplification. The PCR procedure was performed as described in Chapter One. Amplification was examined after electrophoresis on a 1% agarose gel.

DNA sequencing of PCR products. PCR products were purified as described in Chapter One. Since the 1:10 dilute samples yielded the strongest amplification, amplicons from the 1:10 dilution PCRs were purified except for two samples that had the highest amplifications from non-dilute PCR amplicons. Forty nanograms of DNA template was calculated by volume (µl) from each sample based on DNA concentration measurements using a Microvolume UV-Vis Spectrophotometer (Thermo Fisher Scientific NanoDrop One) and added to a 0.2 ml PCR tube. One microliter of primer BGv377 or BGc1509 (10 µM) was added to each tube and the total volume was adjusted to 6.5 µl with molecular grade water.

Sequence analysis and virus identification. Sequence analysis and BLAST searches were performed as described in previous chapters.

RESULTS

***Beet curly top virus* detection.** BCTV capsid protein-coding DNA was detected from all 14 symptomatic hemp samples, but not from the 2 asymptomatic samples. Samples run at a 1:10 DNA dilution yielded higher copies of BCTV PCR amplicons than at original concentrations (Fig. 4-2). Samples 14-16 were received and run after samples 1-13 so we went straight to a 1:10 dilution for PCR as we observed the highest amplification from this concentration from samples 1-13.

All 14 symptomatic samples were detected positive for BCTV by the presence of approximately 1.1 kb of the BCTV capsid protein coding sequence (Fig. 4-2). The healthy plant samples 1 and 2 had no amplification visible from the gel as expected.

Sequence analysis and BLAST search. Sequences of PCR products were obtained for all 14 samples following Sanger sequencing. However, data from 10 samples did not have enough coverage to assemble a full amplicon sequence and their 5' and 3' amplicon sequences were used to perform BLAST searches. BLAST search results confirmed that all 14 DNA samples from the symptomatic hemp plants contained *Beet curly top virus* capsid protein coding sequences (Table 4-1). All the partial amplicon sequences (both 5' and 3') solely hit *Beet curly top virus* and were up to 98% identical to deposited BCTV sequences. Because the sequences were raw data without assembly and edits, some had only 86% sequence similarity to BCTV sequences. However, four

samples (3, 10, 13, and 14) had good sequence data that were assembled to full amplicon sequences. BLAST searches of these full amplicon sequences confirmed their highest similarity (greater than 97%) to available BCTV sequences. Specifically, sample 3 had 1002 bp and was 97.05% identical to *Beet curly top virus* (KX867055, Worland strain); sample 10 had 962 bp and was 98.65% identical to *Beet curly top virus* (MW188519); sample 13 had 995 bp and was 98.08 % identical to *Beet curly top virus* (KX867042, Worland strain); and sample 14 had 973 bp and was 98.98 % identical to *Beet curly top virus* (KX867055, Worland strain).

DISCUSSION

In this study, hemp plants exhibiting symptoms of a viral infection were analyzed for the presence of *Beet curly top virus* (BCTV) capsid protein coding sequences, and we positively detected BCTV from these symptomatic plants. Expectedly, BCTV was not detected from healthy plants. This finding suggests that BCTV is the cause of the disease symptoms expressed in hemp plants. BCTV was reported on hemp in Colorado (Giladi *et al*., 2020) and in Arizona (Hu *et al*., 2020). These positive detections suggest BCTV is a major viral disease of hemp in the western United States.

All sample plants contained BCTV based on partial coding sequences of capsid proteins. However, the lengths of sequences amplified from different plant samples varies significantly, suggesting that the virus detected from each plant or crop may represent different strains. Because BCTV has several forms of strains or variants, and its taxonomy is complex, further studies on the specific strain found from different crops are needed (Rondon, 2016).

Future work for the characterization of BCTV-caused hemp diseases includes further detection of this virus from diverse hemp crops as well as from the beet leaf hopper, the insect vector of BCTV. Information generated from both crops and vectors would help to elucidate the epidemiology of BCTV disease in Nevada. Because BCTV is a complex virus, characterization of each virus strain will help determine which strain is predominant in hemp crops.

Table 4-1. BLAST search results based on 5' and 3' sequences of PCR amplicons (primers 377/1509) generated from 14 symptomatic hemp plants.

Sample ID	BLAST suggested virus (5' sequence)	Accession number	Sequence identity (%)	BLAST suggested virus (3' sequence)	Accession number	Sequence identity (%)
3	*Beet curly top virus*	KX867055	97.67	*Beet curly top virus*	KX867055	96.68
4	*Beet curly top virus*	KT276898	91.79	*Beet curly top virus*	KX867051	94.14
5	*Beet curly top virus*	KX867047	94.43	*Beet curly top virus*	KX867042	87.45
6	*Beet curly top virus*	KX867055	95.25	*Beet curly top virus*	KX867055	96.05
7	*Beet curly top virus*	AY134867	95.47	n/a	n/a	n/a
8	*Beet curly top virus*	KX867051	91.21	*Beet curly top virus*	KX867055	95.09
9	*Beet mild curly top virus*	AY134867	90.95	*Beet curly top virus*	KX867042	99.16
10	*Beet curly top virus*	KX867055	98.20	*Beet curly top virus*	KX867055	98.59
11	*Beet curly top virus*	KX867039	96.59	*Beet curly top virus*	KX867055	94.92
12	*Beet curly top virus*	KX867045	98.40	*Beet curly top virus*	KX867053	86.24
13	*Beet curly top virus*	KX867042	99.11	*Beet curly top virus*	KX867055	89.96
15	*Beet curly top virus*	KX867050	99.72	*Beet curly top virus*	KX867055	99.85
16	*Beet curly top virus*	KX867056	99.56	*Beet curly top virus*	KX867055	98.28
17	*Beet curly top virus*	KX867050	99.58	*Beet curly top virus*	KX867055	96.89

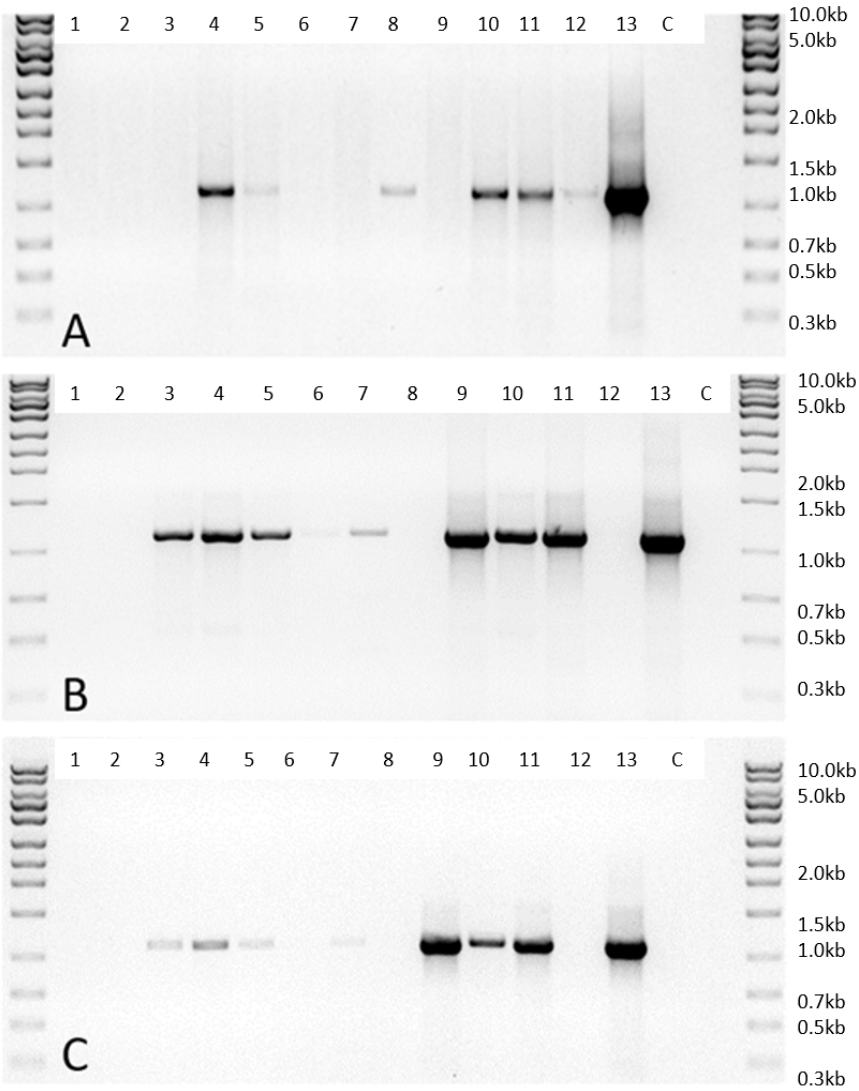

Figure 4-2. PCR amplifications of BCTV capsid protein coding DNA from 11 symptomatic hemp plants and 2 asymptomatic hemp plants using primers 377/1509. Comparison of the same 13 samples run at different dilutions: **A.** non-dilute. **B.** 1:10 dilution. **C.**1:100 dilution. All PCR amplicons were approximately 1.1 kb as expected for BCTV. Wells 3-13: symptomatic samples 1-13, well 14: non-template control. Wells 1 and 2: asymptomatic plant samples. DNA ladder used at the furthest left and right lanes was exACTGene 1kb.

LITERATURE CITED

Bennett, C.W. (1971). *The curly top disease of sugarbeet and other plants*. American Phytopathological Society, St. Paul, MN.

Chen, L. F., & Gilbertson, R. L. (2008). Beet mild curly top virus. Pgs. 195-215 in: *Characterization, Diagnosis & Management of Plant Viruses*. G. P. Rao, S. M. Paul Khurana, and S. Lenardon. Stadium Press, Houston, TX.

Chen, L.-F., Brannigan, K., Clark, R., & Gilbertson, R.L. (2010). Characterization of curtoviruses associated with curly top disease of tomato in California and monitoring for these viruses in beet leafhoppers. *Plant Disease.* 94: 99-108.

Giladi, Y., Hadad, L., Luria, N., Cranshaw, W., Lachman, O. & Dombrovsky, A. (2020). First report of *Beet curly top virus* infecting *Cannabis sativa* in western Colorado. *Plant Disease*. 104:309.

Hu, J., Masson, & R., Dickey, L. (2020). First report of *Beet curly top virus* infecting industrial hemp (*Cannabis sativa*) in Arizona. *Plant Disease*. Epub ahead of print.

Rondon, S. I., Roster, M. S., Hamlin, L. L., Green, K. J., Karasev, A. V., & Crosslin, J. M. (2016). Characterization of Beet curly top virus Strains Circulating in Beet Leafhoppers (Hemiptera: Cicadellidae) in Northeastern Oregon. *Plant disease, 100*(8), 1586–1590.

Soto, M. J., & Gilbertson, R. L. (2003). Distribution and rate of movement of the curtovirus *Beet mild curly top virus* (family *Geminiviridae*) in the beet leafhopper. *Phytopathology*. 93: 478-484.

Strausbaugh, C.A., Eujayl, I.A. & Wintermantel, W.M. (2007). *Beet curly top virus* strains associated with sugar beet in Idaho, Oregon, and a Western U.S. Collection. *Plant Disease*. 101:1373-1382.

Strausbaugh, C. A., Wintermantel, W. M., Gillen, A. M., & Eujayl, I. A. (2008). Curly top survey in the western United States. *Phytopathology*. 98: 1212-1217.

Wintermantel, W. M. (2009). Curly Top. Pgs. 51-53 in: *Compendium of Beet Diseases and Pests*, 2nd ed. R. M. Harveson, L. E. Hanson, and G. L. Hein, eds. American Phytopathological Society, St. Paul, MN.

Chapter Five:

The molecular identification of phytoplasmas associated with witches' broom of hemp based on 16S rDNA sequences.

ABSTRACT

Industrial hemp (*Cannabis sativa* L.) is an emerging crop in Nevada. From 2017 through 2019, industrial hemp crops in Carson City, Lincoln, Lyon, Humboldt, and Nye counties exhibited severe stunting and abnormal growth. Typical symptoms of affected hemp plants were excessive apical branching and crowded growth of underdeveloped leaves, giving a shoot proliferation or clusters of witches' broom appearance. Leaves growing in compact clusters were yellowed, often distorted, and abnormally small in comparison to non-symptomatic sections of the plant or healthy plants of the same variety. These symptoms suggest a phytoplasma infection. Phytoplasma DNA was detected in 14 of the 66 total tested samples with FAM Ct values ranging from 14 to 33. Conventional and nested PCR was then performed using primer pairs P1/P7 and R16F2n/R16R2 (nested), and PCR amplicons of approximately 1.8 kb (PI/P7) and1.2 kb (nested) were obtained. The PCR amplicons were purified, subcloned into pGEM-T vector, and sequenced. DNA sequences of 5'- and 3'- ends of PCR amplicons were obtained. Nucleotide sequence analysis of these sequences confirmed that the phytoplasma obtained in this study was '*Candidatus* Phytoplasma trifolii', a member of the Clover proliferation Group 16SrVI, subgroup 16SrVI-A. While all assembled R16F2n/R16R2 PCR amplicons were more than 99% identical to '*Candidatus* Phytoplasma trifolii' sequences (GenBank accession no. MF092789), sequence data obtained from P1/P7 suggests that some plants may also be infected by *Spiroplasma citri* and other phytoplasmas.

INTRODUCTION

Phytoplasmas are membrane-bound obligate plant parasitic bacteria belonging to the class Mollicutes (Lee *et al.*, 2000). They are transmitted predominately through phloem-feeding insect vectors. Phytoplasmas are known to infect over 700 plant species, many of which are of economic importance (Bertaccini, 2007). Phytoplasma infection often results in devastating crop loss. Symptoms of a phytoplasma infection include yellowing, stunting, witches' broom (shoot proliferation), virescence (green flowers), and phyllody (leaf-like structures growing in place of flowers).

Phytoplasma detection can be difficult due to the current inability to culture phytoplasmas *in vitro*. Further, phytoplasmas are often present in low concentrations (Nejat & Vadamalai, 2013). Identifying phytoplasmas largely relies on PCR methods and sequence data (Hogenhout *et al.*, 2008). Therefore, their classification is based on DNA sequences of the 16S rDNA region (Kumari *et al.,* 2019), by which phytoplasmas are currently classified into many subgroups (Bertaccini & Lee, 2018). However, the phytoplasma organisms are still named in binomial format consisting of a genus name and species name, being named as '*Candidatus* Phytoplasma species.

In 2007, a member of elm yellows phytoplasma group 16SrV was reported from hemp in China (Zhao *et al.*, 2007). In 2008, a member of 16SrI was reported to be associated with witches' broom in India (Raj *et al*., 2008). In 2011, a member of stolbur (16SrXII) group phytoplasma was reported to be associated

with witches' broom disease on *C. sativa* crops in Iran (Sichani *et al.*, 2011). In 2015, a 16Sr XIV-A subgroup associated with witches' broom of *C. sativa* was reported in India (Chaube *et al.*, 2015). In 2018, we detected a phytoplasma closely related to '*Candidatus* Phytoplasma trifolii' from several hemp crops (Schoener & Wang 2019; Wang, 2019). Recently, we noticed a report on *Ca.* P. trifolii found from a *C. sativa* sample from Nevada (Feng *et al*., 2019), which concurs our previous findings.

From 2017 through 2019, a total of 66 hemp samples were collected or submitted to the lab by farmers from Carson City, Lincoln, Lyon, Humboldt, and Nye counties. These samples all exhibited symptoms of severe stunting, leaf yellowing, and clusters of shoot proliferation (Fig. 5-1), all of which are typical of a phytoplasma infection. To elucidate the etiology of this unique disease on hemp, we employed a series of molecular methods to detect and characterize potential phytoplasma species. Information from this research will aid the understanding of the disease biology and epidemiology.

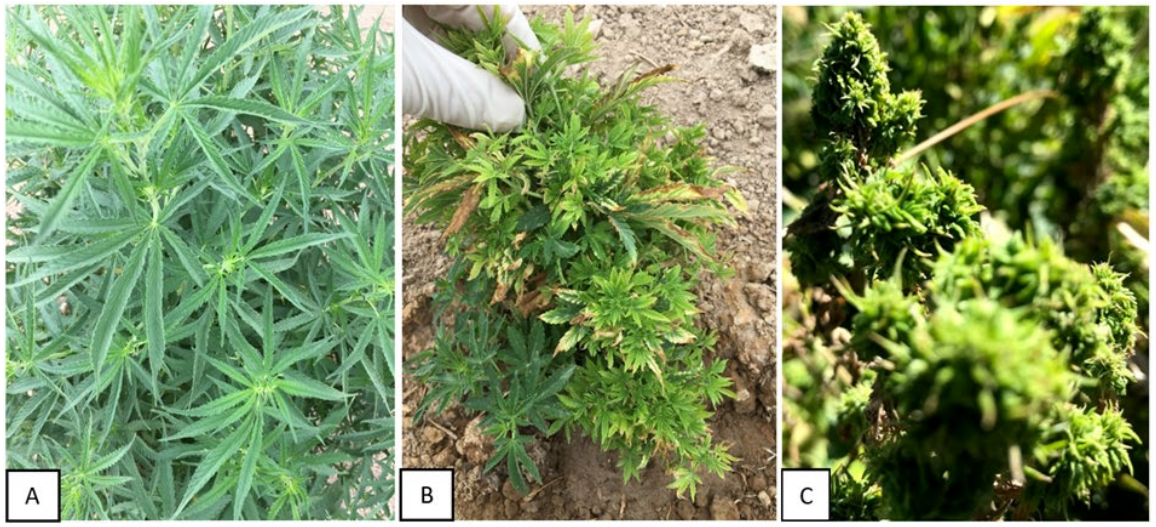

Figure 5-1. Typical symptoms of hemp witches' broom caused by phytoplasmas. A. Healthy hemp plant. **B.** Severe stunting, proliferation, leaf yellowing, and clusters of abnormally small leaves. **C.** Close-up of small, clustered proliferation. (Photo by Shouhua Wang)

MATERIALS AND METHODS

Sample collection and preparation. Hemp plants exhibiting abnormal growth, leaf yellowing, stunting, and witches' broom symptoms were collected by inspectors or submitted by cultivators from Carson City, Humboldt, Lincoln, Lyon, and Nye counties. Upon arrival, a sub-sample (200mg) of midvein and petiole tissue was collected from each symptomatic plant or sample and then proceeded to DNA extraction or stored at -20°C until DNA extraction.

DNA extraction. DNA was extracted from 200 mg of midrib and petiole tissue using Qiagen DNeasy Plant Mini Kit as described in Chapter One with the following modifications: 800 µl buffer AP1 instead of 400 µl, 8 µl RNase A instead of 4 µl, and 260 µl instead of 130 µl buffer P3 were used. The extracted DNA was stored at -20°C.

Phytoplasma detection by multiplex qPCR. A multiplex real-time PCR assay was performed using phytoplasma-specific primers JH-F1/JH-F all/JH-R and probe JH-P uni (Hodgetts *et al.*, 2009). Plant-specific primers (18S F/R) and probe (18S P) were used to detect plant DNA as internal control. The sequences of the primers and probe are listed below:

JH-F 1 (5'-GGTCTCCGAATGGGAAAACC -3')

JH-F all (5'ATTTCCGAATGGGGCAACC -3')

JH-R (5'-CTCGTCACTACTACCRGAATCGTTATTAC -3')

JH-P uni (5'-AACTGAAATATCTAAGTAAC -3')

18S F (5'- GACTACGTCCCTGCCCTTAG-3')

18S R (5’-AACACTTCACCGGACCATTGA -3’)

18S P (5’-ACACACCGCCCGTCGCTC -3’)

The reagents and volumes used for the qPCR reaction were as follows per sample: 15.15 µl of molecular grade water, 2.5 µl of Platinum *Taq* buffer (10X), 3.0 µl of $MgCl_2$ (50 mM), 0.5 µl of dNTP mixture (10 mM), 0.75 µl of primer mix (JH-F 1/JH-F all/JH-R)(10 µM), 0.25 µl of JH-P uni (10 µM), 0.5 µl of primer mix 18S F/18S R (2 µM), 0.25 µl of 18S P (2 µM), and 0.1 µl of Platinum *Taq* polymerase. The qPCR reaction was mixed and 23 µl was added to each 25 µl reaction tube designed for the Cepheid SmartCycler. The DNA template (2 µl), a non-template control (molecular grade water), or a positive control (phytoplasma DNA) was added to each tube. Cepheid tubes were centrifuged and placed into an I-core of a SmartCycler II. The real-time multiplex PCR cycle was run with the following parameters: Stage 1: 95°C for 1 minute with optics off. Stage 2: 40 cycles of 95°C for 5 seconds with optics off and 58°C for 35 seconds with optics on. A sample was considered negative for *Candidatus* Phytoplasma species if it had a FAM Ct value of 0.00 and considered positive if it had a FAM Ct value between 13 and 38.

Nested PCR amplification. All positive samples by qPCR were re-tested with conventional nested PCR to obtain amplicons for sequencing. Primer pair P1/P7 was used to amplify the phytoplasma 16S-23S ribosomal DNA sequence**.** Primer P1: (5’-AAGAGTTTGATCCTGGCTCAGGATT-3’) and primer P7 (5’-CGTCCTTCATCGGCTCTT-3’) (Deng & Hiruki, 1991; Schnieder *et al.*, 1995) are considered as universal primers for phytoplasma. The reagents and volumes

used for the PCR reaction were as follows per sample: 5 µl of Platinum *Taq* buffer (10X), 1.5 µl of $MgCl_2$ (50 mM), 1 µl of dNTP mixture (10 mM), 1 µl of P1 primer (10 µM), 1 µl of P7 primer (10 µM), 0.2 µl of Platinum Taq polymerase, 39.3 µl of molecular biology grade water, and 1 µl of template DNA. One microliter of DNA template for each sample or 1 µl of water (for non-template control) was added to each tube. PCR amplification was performed in a thermocycler with an initial denaturation at 94°C for 2 minutes to completely denature the template DNA and activate the polymerase, followed by 35 cycles of PCR amplification with the following parameters: 94°C for 1 min denaturation, 55°C strand annealing for 2 minutes, and strand extension at 72°C for 3 minutes. A final extension was performed at 72°C for 10 minutes.

Amplicons from the initial P1/P7 PCR were run in a nested PCR with primer set R16F2n (5'-GAAACGACTGCTAAGACTGG -3') and R16R2 (5'-TGACGGGCGGTGTGTACAAACCCCG -3') (Gundersen *et al.*, 1996).
Ten microliters of molecular grade water were added to 1 ul of the P1/P7 PCR product and vortexed to mix. The reagents and volumes used for the PCR reaction were as follows per sample: 5 µl of Platinum *Taq* buffer (10X), 1.5 µl of $MgCl_2$ (50 mM), 1 µl of dNTP mixture (10 mM), 1 µl of R16F2n primer (10 µM), 1 µl of R16R2 primer (10 µM), 0.2 µl of Platinum *Taq* polymerase, 39.3 µl of molecular biology grade water, and 1 µl of template DNA for each sample. PCR amplification was performed under the same parameters as described in the P1/P7 run.

Gel extraction of PCR products. PCR products from P1/P7 and R16F2n/R16R2 runs were loaded to a 1% agarose gel for electrophoresis. The expected band for phytoplasma DNA was cut from the gel and the PCR product was extracted using a Qiagen MinElute Gel Extraction kit. In brief, three volumes of buffer QG were added to one gel weight volume and the mix was incubated at 50°C for 10 minutes with agitation until the gel slice had entirely dissolved. One gel volume of isopropanol was then added to each tube, mixed, added to a QIAquick column, and centrifuged for 1 minute at 13, 000 rpm. Sample flow-through was discarded and 500 µl of buffer QG was added to the column followed by centrifugation for 1 minute at 13, 000 rpm. Sample flow-through was discarded and 750 µl of buffer PE was added to wash the column followed by centrifugation for 1 minute at 13, 000 rpm. After an additional 1 minute centrifugation, the column was then placed into a new1.5 ml microcentrifuge tube to elute DNA with 10 µl of EB buffer. Extracted DNA was stored at -20°C.

Sub-cloning of PCR products via pGEM-T® vector system. Ligation reaction mixture was set up as follows per sample: Five microliters of rapid ligation buffer (2X), 1 µl pGEM-T vector (50 ng), 0.65 or 0.9 µl gel extracted PCR product, 1 µl of T4 DNA ligase (3 Weiss units/ µl), and an amount of molecular grade water to a final volume of 10 µl. The reaction for each sample was mixed by pipetting in 0.2 ml tubes and incubated at 24°C for one hour followed by further incubation overnight at 4°C.

Transformation was performed according to pGEM-T vector system instructions. Briefly, two microliters of each ligation reaction were added to a new

1.5 ml microcentrifuge tube on ice, and 50 µl of Promega JM109 high-efficiency competent cells were added to the tube and gently pipetted to mix. The tube was incubated on ice for 20 minutes, heat-shocked for 45-50 seconds in a 42°C water bath, and then immediately returned into ice for 2 minutes. Nine hundred fifty microliters of room-temperature SOC medium were added to the tube and mixed by pipetting. The mixture was then transferred to a sterile culture tube and incubated at 37°C with shaking at 150 rpm for 1.5 hours. A given volume of cell mixture (30 µl, 70 µl, or 100 µl) was pipetted onto a LB agar plate amended with ampicillin, IPTG, and X-gal, and spread evenly by three sterile glass beads. All plates were incubated at 37°C overnight. Transformed cells grow as white colonies which were picked for plasmid DNA extraction. Five to ten colonies were picked from each sample.

Plasmid DNA extraction. From the culture plate, a single white colony was picked up with the tip of a pipette and expelled the bacterial cells into a culture tube containing the Super Broth amended with 100 µg/ml ampicillin. The tube was incubated at 37°C with shaking at 220 rpm for 16 hours.

Plasmid DNA was extracted using a Qiagen plasmid mini kit**.** Briefly, cells were pipetted into a 1.5 ml microcentrifuge tube and centrifuged for 3 minutes at 8,000 rpm to pellet the bacterial cells. The pellets were resuspended in 250 µl of buffer P1 followed by adding 250 µl of buffer P2. After mixing, 350 µl of buffer N3 was added. The solution was centrifuged at 13, 000 rpm for 10 minutes. The supernatant was pipetted into a QIAprep mini spin column and centrifuged at 13, 000 rpm for 1 minute. Five hundred microliters of buffer PB was added to

columns and centrifuged at 13, 000 rpm for 1 minute. The column was washed twice by adding 750 µl of buffer PE and centrifuging at 13, 000 rpm for 1 minute. Plasmid DNA was eluted from the column by adding 50 µl of buffer EB, and centrifuging at 12, 000 rpm for 1 minute.

Sequencing of Phytoplasma rDNA. For each clone, two hundred fifty nanograms of plasmid DNA and 1 µl of vector primers T7 or SP6 (2 µM) were added into a 0.2 ml PCR tube for Sanger sequencing.

Sequence analysis and BLAST search. Sequence analysis and BLAST searches were performed as described in previous chapters.

RESULTS

Detection of Phytoplasmas by multiplex real-time PCR. Phytoplasma DNA was detected in 14 out of 66 samples with qPCR FAM Ct values ranging from 14 to 33 (Table 5-1). These values were within the FAM threshold (13<x<38) for samples considered to be positive based on qPCR analysis protocol. All 14 positive samples were further analyzed through conventional PCR followed by sequencing.

Amplification of the 16S and 16S-23S spacer region of rDNA and sub-cloning. For all 14 samples with positive FAM qPCR values, conventional PCR generated amplicons of approximately 1.8 kb (PI/P7 primers) and approximately 1.2 kb (R16F2n/R16R2 PCR primers) (Fig. 5-2). Initially, the P1/P7 primer pair amplified an approximate 1.8 kb of 16S rDNA fragment. From these, samples 55, 129, 140, 51, 52, 54, 355, 370, 374, and 378 all generated a strong 1.8 kb band that was gel extracted and sub-cloned. Five clones were selected from each sample for sequencing. Later, all 14 positive samples were further run by nested PCR with primers R16F2n/R16R2, and the amplicons were gel extracted and sub-cloned into the T-vector. Ten clones from each sample were selected for DNA sequencing. Samples 50, 56, and 57 contained double bands and only the expected fragment size (1.2 kb) was purified for sub-cloning. A total of 190 clones were examined for their insert DNA sequences.

Sequence analysis and Phytoplasma identifications. Sequencing the P1/P7 PCR amplicons (samples 51, 52, 54, 55, 129, 140, 355, 370, 374, 378)

cloned into the pGEM-T vector only generated partial 5' and 3' sequences of the 1.8 kb fragment. Of the 50 plasmid DNA samples submitted for sequencing, a total of 30 forward primer (P1) and reverse primer (P7) sequences, were obtained. The remainder of the sequences had insufficient sequence data for comparison. BLAST searches of both P1 and P7-generated sequences suggested that all of them belonged to various strains of '*Ca*. Phytoplasma trifolii' including Iranian cabbage yellows phytoplasma (GenBank accession no. EF592606), accounting for 43.3% of total sequences used for BLAST searches. Other strains such as Columbia Basin potato purple top phytoplasma (GenBank accession no. AY692280) (3%) were also hit by BLAST searches. Sample #129 contains DNA that was over 99% identical to *Spiroplasma citri* (GenBank accession no. CP053304), a serious pathogen distinct but related to phytoplasmas accounted for 10% of P1/P7 sequences used for BLAST searches. BLAST searches of fully assembled R16F2n/R16R2 PCR amplicons (1250 bp) confirmed that all 14 samples contained '*Ca*. Phytoplasma trifolii' (GenBank accession no. MF092789) with 99-100% identical sequence comparison. This result was based on a total of 140 amplicon sequences cloned into the T-vector, 10 from each positive sample, and all of them were nearly identical (Fig. 5-3 and Fig. 5-4).

DISCUSSION

In this study, we used three strategies to detect phytoplasmas in hemp: 1) qPCR to quickly and sensitively detect any strain of phytoplasmas, 2) Nested PCR to examine amplified sequences, and 3) use of cloning to pick multiple clones to detect potentially different phytoplasmas. All these strategies help to find the cause of witches' broom disease in industrial hemp. This study confirmed that '*Candidatus* Phytoplasma trifolii', a member of the clover proliferation group 16SrVI, subgroup 16SrVI-A, is the predominant species responsible for the disease.

By cloning PCR products into a vector, we can examine individual PCR molecules to see if there is potentially a mix of different phytoplasmas present in infected hemp tissue. Initially, only 5 clones were selected from each P1/P7 amplicons during the cloning process. If we examine more clones, there may be more strains of phytoplasmas found.

The P1/P7 amplicons from Sample #129 had greater than 99% sequence identity to that of *Spiroplasma citri*, a mollicute related to phytoplasmas that is known to cause citrus stubborn disease (Saglio *et al.*, 1973). This unique discovery can only be made through cloning strategies. The pathological role of *S. citri* in hemp is unknown.

Due to the highly conserved nature of the 16S rRNA gene, utilizing primers based on this region may not be sufficient to further differentiate closely

related yet distinct phytoplasmas. Potential loci such as *secY* or *tuf* may also be used to identify distinct phytoplasmas (Botti & Bertaccini, 2003; Lee *et al.*, 2006).

While only 14 out of 66 symptomatic hemp plants tested positive for phytoplasma, this could be due to low titers of phytoplasma present in sampled plant tissue as phytoplasmas are known to be found in low concentrations. Additionally, certain viruses may contribute to some symptoms that resemble a phytoplasma infection. We suspect that a virus may be associated with this disease, as we noted that many plants exhibited both witches' broom and leaf mosaic as well as leaf curl symptoms typical to a virus infection. As we have recently detected *Beet curly top virus* (BCTV) from symptomatic hemp plants (described in the previous chapter), we will test all 66 samples used in this study for BCTV. The results may aid in the understanding of the etiology of this devastating hemp disease.

Table 5-1. Identification of phytoplasmas from samples based on full R16F2n/R16R2 PCR amplicon sequences.

Sample ID	qPCR FAM Ct	Sequencing primer pair	Assembled amplicon size (bp)	BLAST suggested Identity	Accession number	Sequence identity (%)
50	31.97	R16F2n/R16R2	1250	Ca.Phytoplasma trifolii	MF092789	99.60
51	18.77	R16F2n/R16R2	1250	Ca.Phytoplasma trifolii	MF092789	100.00
52	14.97	R16F2n/R16R2	1250	Ca.Phytoplasma trifolii	MF092789	100.00
54	16.37	R16F2n/R16R2	1250	Ca.Phytoplasma trifolii	MF092789	100.00
55	18.49	R16F2n/R16R2	1250	Ca.Phytoplasma trifolii	MF092789	100.00
56	17.23	R16F2n/R16R2	1250	Ca.Phytoplasma trifolii	MF092789	100.00
57	32.89	R16F2n/R16R2	1250	Ca.Phytoplasma trifolii	MF092789	99.92
129	28.37	R16F2n/R16R2	1250	Ca.Phytoplasma trifolii	MF092789	100.00
140	23.10	R16F2n/R16R2	1250	Ca.Phytoplasma trifolii	MF092789	100.00
355	18.51	R16F2n/R16R2	1250	Ca.Phytoplasma trifolii	MF092789	99.84
359	27.65	R16F2n/R16R2	1250	Ca.Phytoplasma trifolii	MF092789	99.84
370	24.45	R16F2n/R16R2	1250	Ca.Phytoplasma trifolii	MF092789	100.00
374	18.79	R16F2n/R16R2	1250	Ca.Phytoplasma trifolii	MF092789	99.84
378	17.80	R16F2n/R16R2	1250	Ca.Phytoplasma trifolii	MF092789	99.92

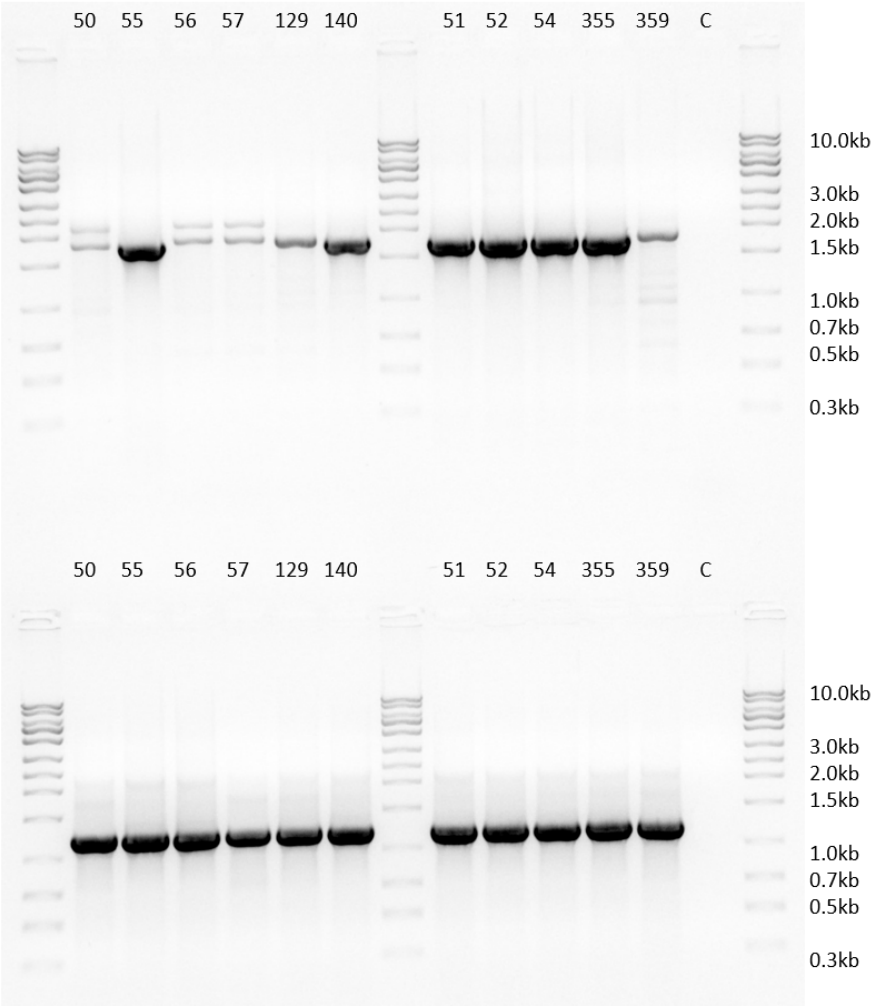

Figure 5-2. Amplification of phytoplasma DNA from symptomatic plants using P1/P7 and R16F2n/R16R2 PCR primer pairs. Lanes are labelled with the sample ID that was loaded. Top gel: PCR with P1/P7 (1.8 kb); bottom gel: nested PCR with R16F2n/R16R2 (1.2 kb). Lane "C": a non-template control. The DNA ladder used was exACTGene 1 kb shown at far left, right and central lanes. Samples 50, 56, and 57 had double banding with P1/P7 and the 1.8 kb fragment was gel extracted for the nested PCR.

Figure 5-3. Sequence alignment of rDNA sequences amplified from 14 hemp samples using Multiple Sequence Comparison by Log- Expectation (MUSCLE). The green regions represent identical sequences.The grey break indicated by the arrow at the bottom of the figure represents the base difference among the sequences. Specific base differences among the sequences are shown in greater detail in Fig. 5-4.

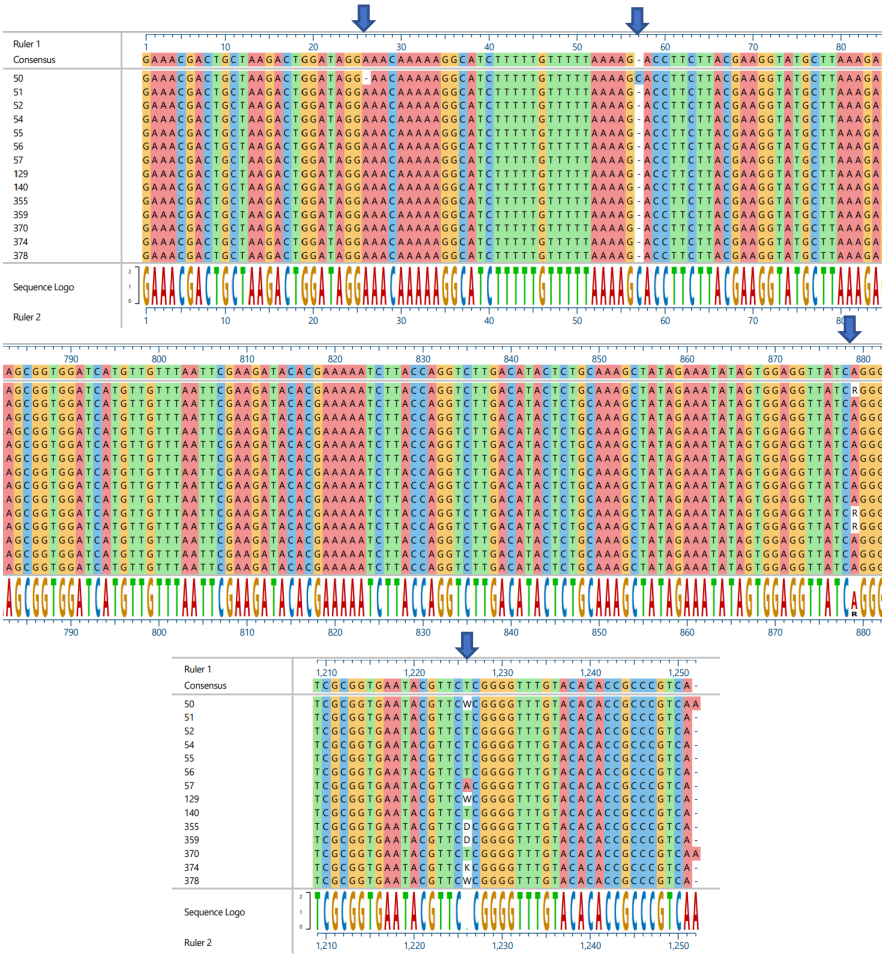

Figure 5-4. Specific base difference among R16F2n/R16R2 PCR amplicon sequences. Blue arrows indicate base differences in sequence data. The ‘W’ in the sequence data represents either adenine or thymine at position 1226 for sequence 50, 129, 378. The ‘D’ in the sequence data represents either guanine or adenine or thymine (not cytosine) for sequences 355 and 359 at position 1226. The ‘R’ in the sequence data represents adenine or guanine at position 879 for sequences 355, 359, and 50. The ‘K’ in the sequence data represents guanine or thymine at position 1226 for sequence 374.The ‘-‘ in the sequence data represents an indel of sequence 50 at positions 26 and 57.

LITERATURE CITED

Bertaccini, A. (2007) Phytoplasmas: diversity, taxonomy, and epidemiology. *Fronters in Bioscience*. 12: 673-689.

Bertaccini, A. & Lee, I.-M. (2018). Phytoplasmas: an update: characterisation and epidemiology of phytoplasma. *Associated Diseases*. 10: 978-981.

Botti, S., & Bertaccini, A. (2003). Variability and functional role of chromosomal sequences in 16SrI-B subgroup phytoplasmas including aster yellows and related strains. *Journal of Applied Microbiology*. 94:103–110.

Deng, S., & Hiruki, C. (1991) Amplification of 16S rRNA genes from culturable and nonculturable mollicutes. *Journal of Microbiological Methods*. 14:53-61.

Feng, X., Kyotani, M., Dubrovsky, S., & Fabritius, A.-L. (2019). First Report of *Candidatus* Phytoplasma trifolii Associated Witches' broom Disease in *Cannabis* sativa in Nevada, U.S.A. *Plant Disease*. 7: 103.

Gundersen, D. E., Lee, I. M., Schaff, D. A., Harrison, N. A., Chang, C. J., Davis, R. E., & Kingsbury, D. T. (1996). Genomic diversity and differentiation among phytoplasma strains in 16S rRNA groups I (aster yellows and related phytoplasmas) and III (X-disease and related phytoplasmas). *International journal of systematic bacteriology*, *46*(1), 64–75. https://doi.org/10.1099/00207713-46-1-64

Hiruki, C., & Wang, K. (2004). Clover proliferation phytoplasma: '*Candidatus* Phytoplasma trifolii'. *International Journal of Systematic and Evolutionary Microbiology*. 54:1349-1353.

Hodgetts, J., Boonham, N., Mumford, R., & Dickinson, M. (2009). Panel of 23S gene-based real-time PCR assays for improved universal and group-specific detection of phytoplasmas. *Applied and Environmental Microbiology*. 75: 2945-2950.

Hogenhout, S.A., Oshima, K., Ammar, E-D., Kakizawa, S., Kingdom, H.N., & Namba, S. (2008). Phytoplasmas: bacteria that manipulate plants and insects. *Molecular Plant Pathology. 9* (4),403–423.

Kumari, S., Nagendran, K., Rai, A.B., Singh, B., Rao, G.P. & Bertaccini, A. (2019). Global status of phytoplasma diseases in vegetable crops. *Frontiers in Microbiology.* 10:1349.

Lee, I. M., Davis, R. E., & Gundersen-Rindal, D. E. (2000) Phytoplasma: phytopathogenic mollicutes. *Annual Review of Microbiology*. 54: 221–255.

Lee, I.M., Zhao, Y., & Bottner, K.D. (2006). SecY gene sequence analysis for finer differentiation of diverse strains in the aster yellows phytoplasma group. *Molecular and Cellular Probes*. 20: 87–91.

Nejat, N., & Vadamalai, G. (2013). Diagnostic techniques for detection of phytoplasma diseases: Past and present. *Journal of Plant Diseases and Protection, 120*(1), 16-25.

Raj, S. K., Snehi, S. K., Khan, M. S., & Kmar, S. (2008). *Candidatus* phytoplasma asteris (group 16SrI) associated with a witches'-broom disease of *Cannabis sativa* in India. *Plant Pathology*. 57:1173-1173.

Saglio, P., Lhospital, M., Lafleche, D., Dupont, G., Bove, J., Tully, & Freundt, E. A.(1973). *Spiroplasma citri* gen. and sp.: A Mycoplasma-like organism associated with "stubborn" disease of citrus. *International Journal of Systematic and Evolutionary Microbiology*. 30:364.

Schnieder, B., Seemüller, E., Smart, C.D., & Kirkpatrick, B.C. (1995). Phylogenetic classification of plant pathogenic mycoplasma-like organisms or phytoplasmas. *Molecular and diagnostic procedures in mycoplasmology.* Academic press. 369-380.

Schoener, J. & Wang, S. First detection of a phytoplasma associated with witches' broom of industrial hemp in the United States. (2019). (Abstr.) *Phytopathology* 109: S2.110.

Sichani, F. V., Bahar, M., & Zirak, L. (2011). Characterization of Stolbur (16SrXII) group phytoplasmas associated with *Cannabis sativa* Witches'-broom disease in Iran. *Plant Pathology Journal. 10*(4),161-167.

Wang, S. (2019). Common marijuana and hemp diseases. *Cannabis Business Times.* 29-38.

Zhao, Y., Sun, Q., Davis, R.E., Lee, I., & Liu, Q. (2007). First report of witches'–broom disease in a *Cannabis* species and its association with a phytoplasma of elm yellows group (16SrV). *Plant Disease*. 91:227.

Conclusion

Section 7501 of the 2018 Farm Bill expands hemp research by including the crop under the Critical Agricultural Materials Act. This provision recognizes the worth and opportunity of hemp and the products that can be derived from it. With the re-emergence and increase of interest in the potential of this crop, it becomes more important to understand how pathogens affect this crop. There is still a lot of unknowns about hemp and the diseases that negatively impact it. This study fills the gap with new knowledge on hemp diseases found in Nevada.

At the molecular level, we have detected and identified several key pathogens in the categories of fungi, viruses, and fastidious bacteria that cause serious diseases in *C. sativa*. While traditional microbiological and pathological approaches are still critical in pathogen detection and characterization, DNA sequence-based approaches are quick, reliable, and more importantly, complement the traditional methods.

Accurate diagnosis of diseases associated with hemp will provide for effective management strategies used to mitigate disease and crop loss. Successful disease management is the key to hemp crop health and production sustainability.